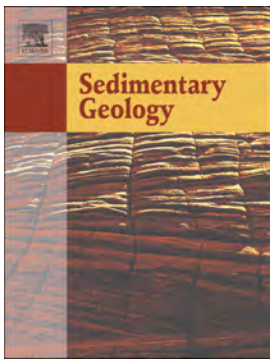

Facies character and skeletal composition of heterozoan carbonates in a high-energy confined embayment (Miocene, Finale Ligure Limestone, NW Italy)

Giovanna Della Porta, Mattia Nembrini, Fabrizio Berra, Agostina Vertino

PII: S0037-0738(22)00130-0

DOI: https://doi.org/10.1016/j.sedgeo.2022.106209

Reference: SEDGEO 106209

To appear in: *Sedimentary Geology*

Received date: 30 May 2022

Revised date: 5 July 2022

Accepted date: 6 July 2022

Please cite this article as: G.D. Porta, M. Nembrini, F. Berra, et al., Facies character and skeletal composition of heterozoan carbonates in a high-energy confined embayment (Miocene, Finale Ligure Limestone, NW Italy), *Sedimentary Geology* (2022), https://doi.org/10.1016/j.sedgeo.2022.106209

Facies character and skeletal composition of heterozoan carbonates in a high-energy confined embayment (Miocene, Finale Ligure Limestone, NW Italy)

Giovanna Della Porta[1], Mattia Nembrini[1], Fabrizio Berra[1], Agostina Vertino[2]

[1]Università degli Studi di Milano, Dipartimento di Scienze della Terra "A. Desio", via Mangiagalli 34, 20133 Milan, Italy. E-mail: giovanna.dellaporta@unimi.it; mattia.nembrini@unimi.it; fabrizio.berra@unimi.it

[2]Department of Geology, Ghent University, Campus Sterre, Building S8, Krijgslaan 281, B-9000 Gent, Belgium. Email: agostina.vertino@ugent.be

ABSTRACT

During the early and middle Miocene, diverse photozoan to heterozoan carbonate and mixed carbonate-siliciclastic depositional systems characterized the Mediterranean region at palaeo-latitudes of 30-40°N, during a time of warm climate. These systems ranged from carbonate ramp to rimmed platforms to current-swept flooded incised palaeo-valleys, seaways and straits. This study focuses on the facies character, skeletal biota composition, diagenesis and stable carbon and oxygen isotopic signature of a mixed carbonate-siliciclastic succession (lower-middle Miocene Finale Ligure Limestone and underlying Oligocene-lower Miocene siliciclastic deposits) accumulated in a high-energy coastal setting (Finale Ligure, NW Italy) to improve the knowledge on the variety and controlling factors of Miocene heterozoan skeletal carbonates.

The 3D reconstruction of the geometry of the early-middle Miocene Finale Ligure basin identifies an embayment, about 35 km^2 wide, limited by uplifted and eroded Alpine tectonic units and connected to the open sea through a strait. The Oligocene-Miocene sedimentary succession unconformably overlying the Alpine deformed substrate consists of 14 lithofacies (L1-L14). Besides pockets of karstic breccias (L1) preceding the marine transgression, discontinuous outcrops

of glaucony-bearing litharenite, siltstone, conglomerate and wackestone/packstone with planktonic foraminifera (L2-L4) represent the preserved remnants of an eroded marine shelf affected by tectonic uplift and subsequent erosion, approximately in the Aquitanian-Burdigalian, overlain through an angular unconformity by transgressive conglomerates and bioturbated litharenites (L5-L7). The onset of carbonate skeletal production characterizes the overlying compositionally mixed carbonate-siliciclastic Finale Ligure Limestone succession (up to 100-150 m thick, L8-L14). These cross-bedded skeletal packstone and grainstone/rudstone are composed of barnacles, echinoderms, bryozoans, bivalves, scleractinian and stylasterid corals, and lack halimedacean algae as previously published. They accumulated in a high-energy setting with strong bottom currents, driven by the amplification of tidal and/or storm currents in a confined embayment, promoting the formation of seaward prograding metre-scale subaqueous dunes.

Unlike other lower-middle Miocene carbonate systems, the Finale Ligure heterozoan carbonates contain rare coralline red algae and larger benthic foraminifera but are enriched in barnacles, scleractinian and stylasterid corals. The coastal palaeo-environmental conditions, with hard rocky substrates, strong bottom currents, high nutrient and water turbidity, influenced the composition of the skeletal carbonate producers. These distinctive lithofacies character and composition resulted from the confined embayment morphology inherited from the marine flooded Alpine bedrock that was subjected to land runoff driving nutrient input.

Keywords: Miocene; Finale Ligure; heterozoan carbonates; embayment; subaqueous dunes; stylasterid corals

1. Introduction

Diverse carbonate and mixed carbonate-siliciclastic depositional systems developed in the Mediterranean region during the Miocene (Carannante et al., 1988; Pedley, 1998; Pomar et al., 2004, 2017; Brandano et al., 2017a; Michel et al., 2018; Cornacchia et al., 2021 and references

therein). Miocene carbonate-producing skeletal biota ranged from the heterozoan association (light independent heterotrophic biota, including molluscs, echinoderms, barnacles, bryozoans, brachiopods and foraminifera associated with red algae; *sensu* James, 1997) to the photozoan association (light dependent zooxanthellate corals and green algae; *sensu* James, 1997), under the control of basin physiography, palaeoceanography, seawater circulation patterns, nutrient levels, siliciclastic input, hydrodynamic energy, salinity, oxygen levels, water turbidity, water depth and temperature (Mutti and Hallock, 2003; Pomar et al., 2004; Halfar et al., 2004; Halfar and Mutti, 2005; Wilson and Vecsei, 2005; Pomar and Hallock, 2007; Westphal et al., 2010; Perrin and Bosellini, 2012; Pomar et al., 2012; James et al., 2014; Brandano et al., 2017ab; Coletti et al., 2017; Pomar et al., 2017; Cornacchia et al., 2018, 2021). These Mediterranean Miocene sedimentary successions were deposited in tectonically active geodynamic scenarios, at palaeo-latitudes around 30-40° N (Fig. 1A; Dewey et al., 1989; Gueguen et al., 1998; Dercourt et al., 2000; Popov et al., 2004). Climate conditions are suggested to have varied from a late Oligocene to early Miocene (Aquitanian) warming trend, interrupted by brief glaciation events, to a mid-Miocene climatic optimum across Burdigalian to Langhian times (approximately 17-14.5 Myrs), followed by a cooling trend from the Serravallian (Zachos et al., 2001; Mosbrugger et al., 2005; You et al., 2009; Billups and Scheiderich, 2010; Brandano et al., 2017b; Cornacchia et al., 2021; Drury et al., 2021).

The interplay between heterozoan, photozoan and transitional carbonate factories, processes of sediment transport and accumulation and the local environmental and tectonic settings affects sediment composition, facies character, architecture and the geometry of the depositional profile (Halfar et al., 2006; Pomar and Kendall, 2008; Chiarella and Longhitano, 2012; Pomar et al., 2012; Chiarella et al., 2019). Accordingly, Miocene Mediterranean carbonate depositional systems varied from mainly heterozoan carbonate ramps (Betzler et al., 1997; Pedley 1998; Brandano and Corda, 2002; Pomar et al., 2002; Pedley and Carannante, 2006; Knoerich and Mutti, 2003, 2006ab; Mateu-Vicens et al., 2008; Brandano et al., 2016, 2017a; Michel et al., 2018) to photozoan dominated high-relief rimmed platforms (from late Tortonian; Pomar et al., 1996, 2002, 2012, 2017) to

heterozoan carbonate ramps evolving into photozoan flat-topped platforms (Benisek et al., 2009; Tomas et al., 2010; Andreucci et al., 2017). In the Mediterranean region, an additional category of Miocene heterozoan carbonate and mixed siliciclastic-carbonate systems was represented by straits, seaways and embayments in flooded incised palaeo-valleys (Michel et al., 2018) as those identified in southern Spain (North Betic Strait, Martín et al., 2001, 2009; Braga et al., 2010), Corsica (Bonifacio Strait, André et al., 2011; Reynaud et al., 2013; Saint-Florent Basin, Brandano and Ronca, 2014), Sardinia (Longhitano et al., 2017; Telasca et al., 2020) and southern France (Reynaud et al., 2006; Reynaud and James, 2012; James et al., 2014; Coletti et al., 2017, 2018ab).

Among the facies models for heterozoan carbonates, James and Lukasik (2010) identified seaways and embayments as a distinct category differentiated from open ocean shelves and interior basin ramps because seaways, straits and embayments are considered as unique depositional settings dominated by currents (Dalrymple, 2010). The knowledge on the distinctive sedimentological features of these current-swept systems has been considerably expanded in the last decade, in particular through the investigation of Cenozoic deposits in the Mediterranean region (Longhitano, 2011, 2013, 2018ab; Chiarella and Longhitano, 2012; Longhitano et al., 2012ab, 2021ab and references therein). These depositional settings form where conditions are optimum for tidal or unidirectional current acceleration such as in ocean straits, passages between islands, seaways and flooded incised palaeo-valleys. In these settings, several metre-scale subaqueous cross-bedded sand dunes made of heterozoan carbonate grainstone and rudstone with coralline algae and variable amounts of terrigenous clastics form in water depths of few to several tens of metres (e.g., dunes ca. 9 m high in 40-60 m water depth according to Anastas et al., 2006; James and Lukasik, 2010; dunes 10 m in 70 m water depth according to Andrè et al., 2011 and Reynaud et al., 2013 based on Yalin, 1964). Coastal environments where sea-level rise floods an inherited topography can result in confined embayments with amplification of tidal or unidirectional currents, characterized by sedimentological features that place them outside the usual set of carbonate depositional systems (James et al., 2014). In these settings, sediments have different origin, both

intrabasinal, sourced by diverse carbonate factories inside the flooded palaeotopography and from the open sea, and extrabasinal, from the erosion of surrounding incised lithologies (James and Lukasik, 2010). The narrow flooded paleao-valleys favour the development of strong tidal currents that generate a suite of carbonate bedforms, some of which are unique in carbonate depositional systems (James et al., 2014). To improve the knowledge on facies character and skeletal composition of carbonates developed in current-swept seaways and embayments in the Mediterranean region during the Miocene, this study investigates the lower-middle Miocene succession of the Finale Ligure Limestone, also known as Pietra di Finale (Boni et al., 1968; Dallagiovanna et al., 2011; Brandano et al., 2015), preserved along the north-western Italian coast of the Ligurian Alps, close to the town of Finale Ligure (Figs. 1B, 2). These cross-stratified compositionally mixed (*sensu* Chiarella et al., 2017) carbonate-siliciclastic deposits (Fig. 3) consist of skeletal carbonates with variable abundances of detrital grains, unconformably overlying siliciclastic Oligocene to lower Miocene strata or the Alpine tectonic units consisting of deformed Paleozoic-Mesozoic successions (Boni et al., 1968, 1971). The Finale Ligure Limestone skeletal grainstone-rudstone strata were interpreted as deposited in a shallow-marine, nutrient-enriched prograding coastal wedge with common halimedacean algae (Brandano et al., 2015). The detailed characterization of the skeletal composition and the depositional model presented here expand and better document the interpretation by Nembrini et al. (2017) that the Finale Ligure Limestone heterozoan carbonates, dominated by barnacles, bryozoans, molluscs, scleractinian and stylasterid corals, formed metre-scale subaqueous dunes accumulated in a kilometre-scale confined embayment. This study contributes to the current knowledge on the diversity of depositional systems in the Mediterranean region during the Miocene and expands the understanding of high-energy heterozoan carbonates filling flooded Alpine palaeotopography.

2. Geological Setting

2.1 Tectonic setting

During the Oligocene and Miocene, the western Mediterranean region was affected by active tectonics due to the relative movements of Africa, Europe and minor plates, with the coexistence of compressional and extensional regimes (Alvarez, 1976; Dewey et al., 1989; Carminati et al., 1998). Following the Alpine Orogeny, extension took place in the western Mediterranean during the late Oligocene-early Miocene, leading to the opening of back-arc basins (Rehault et al., 1984; Stampfli and Marchant, 1997; Carminati et al., 1998; Gueguen et al., 1998; Carminati and Doglioni, 2005): Alboran, Valencia Trough, Algerian and Ligurian Provençal Basin (Fig. 1A), which originated by the 30° counter clockwise rotation of the Sardinia-Corsica microplate (Speranza et al., 2002). A second extensional phase (from the Tortonian time to present) led to the formation of the Tyrrhenian Basin (Malinverno and Ryan, 1986; Carminati et al., 1998). In this geodynamic scenario, diverse Miocene sedimentary successions were deposited in various tectonically-controlled settings and on inherited topography. The carbonate-siliciclastic sedimentary succession under investigation in the area of Finale Ligure accumulated at the northern border of the Ligurian Provençal Basin (Fig. 1A-B).

The tectonic regime affecting the Finale Ligure study area can be derived from the evolution of the Tertiary Piedmont Basin (TPB), located North of Finale Ligure (Fig. 1B). During the Oligocene-Miocene, the TPB recorded three tectonic events: 1) exhumation of the Alpine Briançonnais domain during the Rupelian-early Chattian, controlled by NNW-striking fault systems, related to a brittle deformation phase (Maino et al., 2013), with marine transgression driven by moderate subsidence associated with the development of extensional faults (Mutti et al., 1995; Maino et al., 2013); 2) onset of syn-sedimentary faults during the late Chattian in a sinistral strike-slip transtensional regime; 3) development of open folds in the TPB and in the metamorphic basement during the early Miocene (Aquitanian-early Burdigalian). These early Miocene compressional structures (Fig. 1B), post-dating the Oligocene transtensional tectonics, are

indicative of NE-SW shortening (Maino et al., 2013). A transpressional regime is also documented by positive flower structures near the Villalvernia-Varzi line (Mosca et al., 2010), NE of Finale Ligure (Fig. 1B) and in the eastern Monferrato area (NW of TPB and Finale Ligure), where it resulted in an angular unconformity between Aquitanian and Burdigalian strata (Clari et al., 1995; Coletti et al., 2017). The middle Miocene (Langhian-Serravallian) sedimentary successions in the TPB display NE-SW oriented extensional and NW-trending contractional structures, with limited displacement (Maino et al., 2013). During the late Burdigalian-Serravallian, an increase in subsidence rate over the entire TPB is explained by flexural response to thrust loading (Carrapa et al., 2003).

2.2 Stratigraphic framework

The investigated Oligocene-Miocene sedimentary succession in the Finale Ligure area, overlies the deformed Alpine Briançonnais units of the Ligurian Alps (Figs. 1-3), which consist of metamorphic, Carboniferous to Jurassic metavolcanic and metasedimentary rocks (Boni et al., 1971; Dallagiovanna et al., 2011). The Briançonnais units comprise the Triassic to Eocene S. Pietro dei Monti Dolostone, Val Tanarello Limestone and Caprauna Formation (Fig. 4), unconformably overlain by Oligocene to Miocene siliciclastic and mixed carbonate-siliciclastic strata, including the lower-middle Miocene Finale Ligure Limestone (Calcare di Finale Ligure; "Pietra di Finale" *Auct*.; Boni et al., 1968, 1971; Dallagiovanna et al., 2011; Fig. 2A), also labelled as Pietra di Finale Formation (Brandano et al., 2015; Fig. 2B). The siliciclastic deposits comprised between the Alpine units and the Finale Ligure Limestone have been defined as "Basal Complex" of the Finale Ligure Limestone by Boni et al. (1971) and include four units (Fig. 2A): 1) polygenic conglomerate and sandstone; 2) monogenic breccia with clasts of the Triassic S. Pietro dei Monti Dolostone (Borgio Breccia in Figure 2A); 3) coarse sandstone and fine-grained, quartz-rich conglomerate with centimetre-thick intercalations of green claystone and marlstone (Sandstones and Marls, West of

Mt. Cucco); 4) grey-yellow claystone, siltstone and marlstone (S. Lorenzino Marls). The age of these deposits is suggested to be early Oligocene (Mosna et al., 1990) to probably early Miocene (Aquitanian-Burdigalian) for the Marls West of Mt. Cucco (Boni et al., 1968, 1971). The stratigraphic relationships among these sedimentary units are difficult to reconstruct because of limited and discontinuous outcrop exposures (Boni et al., 1968). The Finale Ligure Limestone, which is unconformably transgressive either on the Alpine bedrock or on the "Basal Complex", consists of five members (Fig. 2A; Boni et al., 1968, 1971). The two discontinuous basal members (marlstone and sandstone of the Torre di Bastia Mb. and conglomerate of the Poggio Mb.) are siliciclastic deposits, attributed to Aquitanian-Burdigalian to probably basal Langhian (Boni et al., 1968). The overlying three members (Verezzi, Rocce dell'Orera and Monte Cucco members) are dominated by carbonate skeletal fragments and are suggested to be Langhian-Serravallian in age by Boni et al. (1968, 1971). According to Boni et al. (1968, 1971), the Verezzi Mb. (about 50 m thick) is a red-colour skeletal calcarenite with pectinid and oyster bivalves, echinoids, corals, brachiopods and rare shark teeth associated with siliciclastic detrital grains. The Rocce dell'Orera Mb. (70 m thick) overlies the Verezzi Mb. through an erosional surface and consists of hybrid sandstones rich in fragments of corals, algae, molluscs, bryozoans and balanids, with interbedded polygenic conglomerates with clasts of Permian and Triassic rocks. The Monte Cucco Mb. (nearly 200 m thick) is a skeletal limestone with scarce terrigenous fraction, with abundant fragments of oysters, balanids, corals, *Halimeda* algae, bryozoans and brachiopods. Boni et al. (1968) interpreted the Finale Ligure Limestone as deposited in an epineritic environment, a marine gulf only partially connected to the open sea, with agitated, warm, shallow waters and reduced terrigenous sediment supply.

Brandano et al. (2015) subdivided the Finale Ligure Limestone (labelled as Pietra di Finale Fm.) into two units (Fig. 2B): the terrigenous unit (Aquitanian-Burdigalian), which comprises the Poggio Mb. and the Torre di Bastia Mb. of Boni et al. (1968), and the calcareous unit (Langhian-Serravallian), consisting of five sedimentary facies. The calcareous unit includes two conglomerate

facies (F1 crudely bedded, F2 cross-bedded), with clasts derived from the Alpine dolostone and metamorphic bedrock associated with skeletal grains (balanids, echinoids, bivalves, bryozoans and rare *Amphistegina* foraminifera). The other three calcareous facies are distinguished on the basis of the dominant skeletal components: the balanid facies (F3) consists of cross-bedded, balanid-rich floatstone to rudstone in a coarse hybrid grainstone matrix; the *Halimeda* facies (F4) is represented by cross-bedded *Halimeda* calcareous algae floatstone to rudstone; the bivalve facies (F5) is a floatstone with sandstone matrix and locally cross-bedding. Brandano et al. (2015) interpreted the Finale Ligure Limestone as a coastal wedge developed along the depositional dip direction of a mixed carbonate-siliciclastic system. The F1 and F2 conglomerates are interpreted as indicative of shoreface depositional environments (Fig. 2B) fed by ephemeral streams and coastal erosional processes. The balanid-rich facies F3 accumulated in high-energy shoreface settings and graded from shoreface to the offshore transition zone, where the *Halimeda* and *Porites* coral-rich facies dominated (F4). The pectinid bivalve floatstone facies (F5) was considered to represent the offshore zone with decreased hydrodynamic energy. According to Brandano et al. (2015), the coral and *Halimeda*-rich photozoan carbonate association (F4) replaced the seagrass meadows carbonate production, which is the common euphotic zone facies in the Mediterranean area in oligotrophic to low mesotrophic conditions from the Miocene to Recent (Mateu-Vicens et al., 2008, 2012). Brandano et al. (2015) suggested that the *Halimeda* growth might have outcompeted the development of seagrass meadows, favoured by increased nutrients due to continental siliciclastic input in the Finale Ligure coastal setting.

Recently, a review of the geological and geomorphological framework of the Finale Ligure Limestone (Bonci et al., 2019a) and the key features in terms of facies character, paleontological content and petrophysical properties (Arobba et al., 2019; Bonci et al., 2019b; Bonino, 2019) were summarised in an edited volume evaluating also the quarrying activities and the cultural heritage of this lithostratigraphic unit (Murialdo et al., 2019). Baucon et al. (2020) investigated the trace fossils belonging to the Verezzi Member observed on buildings made of the Finale Ligure Limestone.

3. Methods

The spatial distribution and sedimentological characteristics of the Finale Ligure Limestone and underlying Oligocene-lower Miocene terrigenous strata were investigated through geological mapping at the 1:10,000 scale and the production of a geological map in a GIS database (Fig. 4), logging of 10 stratigraphic sections and petrographic analysis of 98 thin sections. Facies characterization in terms of texture and grain composition allowed distinguishing 14 lithofacies types (Table 1, 2). Field data, integrated with a network of geological cross sections (Fig. 5), provided the constraints for the reconstruction of the 3D geometry of the Finale Ligure sedimentary basin through the interpolation of lithological boundaries, aiming at the reconstruction of the pre-depositional topographic surface using the software MOVE™.

Twenty-three polished thin sections were examined under cathodoluminescence microscopy with a luminoscope Cambridge Image Technology Limited (CITL), Cambridge, UK (model MK 5-2 operating system at 10-16 kV with a beam current between 200-400 μA, and vacuum gauge 50-70 millitor). Six suitable samples of poorly consolidated marlstone and sandstone were processed for biostratigraphic analysis of planktonic and benthic foraminifera. Samples were mechanically broken and treated with H_2O_2 (5 %) for about 15 hours, then processed using sieves with mesh size of 350 μm, 250 μm, 125 μm and 64 μm. The four fractions were dried and then observed with a stereoscopic microscope.

Stable oxygen and carbon isotope analyses of 66 samples (Table S1 in Supplementary Data online) were performed using an automated carbonate preparation device (Gasbench II) and a Thermo Fisher Scientific Delta V Advantage continuous flow mass spectrometer at the Department of Earth Sciences, University of Milan. Carbonate powder samples, extracted with a microdrill, were reacted with > 99% orthophosphoric acid at 70°C. The carbon and oxygen isotope compositions are expressed in the conventional delta notation calibrated to the Vienna Pee-Dee

Belemnite (V-PDB) scale by the international standards IAEA 603 and NBS-18. Analytical reproducibility for these analyses was better than ± 0.1‰ for both $\delta^{18}O$ and $\delta^{13}C$ values.

4. Results

4.1 Lithofacies character and spatial distribution

Geological mapping, cross-sections and stratigraphic logging (Figs. 3-6) permitted the identification of 14 lithofacies types (Table 1, 2) in the Oligocene-Miocene succession overlying the Alpine tectonic units in the Finale Ligure area. Lithofacies L1 to L7 are terrigenous, mostly siliciclastic deposits sourced by the Alpine bedrock, with absent to sparse carbonate skeletal grains, corresponding to the "Basal Complex" of the Finale Ligure Limestone according to Boni et al. (1968, 1971) or to the Cenozoic substrate and the terrigenous unit of the Pietra di Finale Fm. (Fig. 2), following Brandano et al. (2015). The depositional architectures of these lithofacies are difficult to reconstruct because of the limited lateral continuity of outcrop exposure (Figs. 4, 5). Lithofacies L8 to L14 are compositionally mixed skeletal carbonate-siliciclastic deposits extending across the entire Finale Ligure study area (Figs. 3, 4) belonging to the calcareous unit (Monte Cucco, Rocce dell'Orera, Verezzi members; Fig. 2) of the Finale Ligure Limestone.

The identified 14 lithofacies are gathered in three groups on the basis of sedimentological characteristics, stratigraphic position and spatial distribution, labelled as stratigraphically lower, intermediate and upper lithofacies group. The stratigraphically lower group includes lithofacies L1 to L4 (Table 1) cropping out in discontinuous units, comprised between a basal non-conformity with the underlying Alpine bedrock and an upper erosional and angular unconformity separating this lower lithofacies group L1 to L4 from the succession L5 to L14. Lithofacies L1 consists of up to 100 m thick, massive monomictic clast-supported breccia (Fig. 7A) with clasts derived from the Triassic S. Pietro dei Monti Dolostone (Fig. 4). Lithofacies L2 is a glaucony-bearing litharenite

(Fig. 7B), up to 15 m thick, with sparse planktonic foraminifera, alternating with conglomerate beds. Lithofacies L3 includes 30 m of alternating litharenite and siltstone (L3.1) and laminated packstone-wackestone to fine-grained litharenite beds (L3.2) with planktonic and benthic foraminifera and brachiopods (Fig. 7C-E). Lithofacies L4 (1-20 m thick) consists of litharenite, siltstone and laminated claystone and marlstone beds (Fig. 7F). Lithofacies L1 to L3 crop out only in the SW outcrop area of Verezzi, between Bracciale and Mt. Caprazoppa, whereas lithofacies L4 occurs only in the northern outcrops of Mt. Cucco, near San Lorenzino and Rocca Carpanea (Figs. 4, 5). West of Mt. Cucco, an angular unconformity occurs between L4 litharenite and claystone and the overlying skeletal grainstone/rudstone (L14) of the Finale Ligure Limestone (Figs. 4, 5, 8A). North of Mt. Cucco, at San Lorenzino, an erosional unconformity separates lithofacies L4 from the overlying L5 conglomerate and breccia (Fig. 6, 8B-C).

The stratigraphically intermediate lithofacies group includes L5, L6 and L7 (Table 2) representing laterally discontinuous, coarse grained conglomerate, breccia and litharenite beds that overlie either the deformed Alpine bedrock or lithofacies L1 and L4 at the northern and southern margins of the Finale Ligure Limestone outcrops (Figs. 4, 5). In the North (San Lorenzino; Fig. 6) lithofacies L5 consists of conglomerate, breccia and litharenite with clasts from the Alpine bedrock (3.5 m thick) overlying L4 through an erosional unconformity (Fig. 8B-C). Lithofacies L6 consists of 30-40 m thick (Fig. 6) well-cemented conglomerate followed by burrowed litharenite (Fig. 9A-B) overlying the metamorphic Alpine substrate in the W and S (Rocca di Perti, S. Eusebio and Rocca di Corno; Figs. 4-6). L6 is overlain through a sharp, slightly erosional, contact by L8 bedded litharenite and conglomerate with abundant skeletal fragments (Figs. 6, 9A). Lithofacies L7 (50 m thick) consists of well-cemented conglomerate and litharenite with glaucony directly overlying the Alpine bedrock or L1 (Fig. 9C-D), cropping out only in the SW Verezzi area, between Poggio and Mt. Caprazoppa (Figs. 4-6). As for L6, an erosional surface separates L7 from the overlying lithofacies L8 (Fig. 6).

The stratigraphically upper lithofacies group includes the compositionally mixed carbonate-siliciclastic lithofacies (L8-L14) that are characterized by sparse (L8, L9) to dominant (L10-L14) skeletal fragments (Table 2). These skeletal packstone and grainstone/rudstone strata onlap the Alpine bedrock (Figs. 3-5) in the northern, south-western and south-eastern parts of the Finale Ligure Limestone area or overlie lithofacies L2, L3 and L4 through erosional and angular unconformities or lithofacies L5-L7 through sharp erosional contacts (Fig. 6). Lithofacies L8 includes conglomerate and immature litharenite (from 10 cm to 30 m thick) with quartz, metamorphic and carbonate rock fragments and sparse skeletal fragments, such as brachiopods, bivalves, bryozoans, barnacles, echinoderms and textularid foraminifera (Fig. 9E). Lithofacies L8 mostly occurs: a) at the base of the Finale Ligure Limestone calcareous succession (lithofacies L12-L14), either directly in contact with the Alpine bedrock or overlying lithofacies L6 or L7 (Figs. 4-6), and b) in decimetre to metre thick beds alternating with lithofacies L13 and 14 (Figs. 4, 6). L9 consists of beds of immature matrix-supported litharenites (2-4 m thick) with planktonic and textularid foraminifera filled by glaucony (Fig. 9F), intraclasts and erosional discontinuity stained with Fe oxide. Lithofacies L10 is 5-15 m thick and characterized by decimetre-thick tabular cross-bedded packstone/grainstone to rudstone with locally bidirectional cross-lamination, rich in pectinid bivalves associated with barnacles, bryozoans, echinoderms, sparse to rare benthic and planktonic foraminifera, detrital grains and glaucony pellets (Fig. 10A-B). Lithofacies L11 is a 2 m thick, red in colour, skeletal packstone with common planktonic (*Globigerinoides, Praeorbulina, Orbulina universa*) and rare benthic (*Amphistegina, Elphidium*, textularids, nodosarids, miliolids) foraminifera associated with abraded fragments of bivalves, barnacles, brachiopods, bryozoans and rare coralline red algae (Fig. 10C-D). Fe oxide stained micrite and crusts of laminar calcrete with quartz detrital grains occur within L11 skeletal packstone (Fig. 10C). Lithofacies L12 consists of decimetre- to metre-thick cross-bedded skeletal packstone to rudstone dominated by bivalves, echinoderms, bryozoans, barnacles and brachiopods with rare benthic foraminifera, rare scleractinian and stylasterid corals, red algae fragments and detrital siliciclastic grains (Figs. 10E-F,

11A). Cross-bedded grainstone to rudstone dominated by barnacles associated with echinoderms, bryozoans, bivalves and rare scleractinian and stylasterid corals characterise lithofacies L13 (Fig. 11B-C). Lithofacies L14 consists of cross-bedded skeletal grainstone to rudstone with common scleractinian and stylasterid corals (Figs. 11D-H, 12A-H, 13A-C) associated with barnacles, echinoderms, bivalves (in particular oyster shells affected by microborings) and bryozoans. Lithofacies L12, L13 and L14 display an array of cross-bedded sedimentary structures at several metres to decimetre-scale including compound tabular cross-bedding, planar and trough cross-lamination dipping in multiple directions but prevalently southward (seaward), flaser and wavy bedding associated with sharp erosional surfaces separating the tabular cross beds (Figs. 3B-C, 11D-H). In the Rocca di Perti, Rocca Carpanea and Mt. Cucco-Rocca di Corno outcrop areas, the Finale Ligure Limestone skeletal strata include lithofacies L8 and L12-L14, with dominant L14 (Figs. 4-6) alternating with decimetre-scale beds of L8 reaching up to 150 m in thickness in the Mt. Cucco-Bric Spaventaggi central area (Figs. 4-6). In the SW Verezzi area, the skeletal carbonate succession of the Finale Ligure Limestone comprises lithofacies L8 to L13 (Figs. 5, 6), with a maximum thickness of nearly 100 m (Figs. 4-6).

4.2 Diagenetic features and stable carbon and oxygen isotopes

The investigated lithofacies show different diagenetic features as summarised in Table 1 and 2. In the terrigenous lithofacies L1 to L7, mechanical and chemical compaction (e.g.; grain breakage, elongated, concavo-convex and sutured grain contacts, stylolites) predates cementation by non-luminescent blocky sparite. Burrows are differentially cemented by blocky calcite in lithofacies L6 (Fig. 9A-B). Silicification is common in L3 (Fig. 7E) with chalcedony filling pores and replacing calcite shells (foraminifera and brachiopods). In the calcareous unit of the Finale Ligure Limestone, L12, L13 and L14 packstone/grainstone and rudstone are partially cemented by non-luminescent isopachous fibrous to bladed cement before mechanical compaction followed by

blocky sparite or by scalenohedral cement coated by Fe oxides in the open pore space (Fig. 12F, 13A-C). In L12 packstone, isopachous rims of fibrous cement predate the sedimentation of micrite in the interparticle space (Fig. 13D). In lithofacies L12, L13 and L14, inter- and intraparticle porosity is associated with mouldic and vuggy porosity (Fig. 13A-C), documenting dissolution of both aragonitic and calcitic skeletal fragments. Barnacle biomoulds are filled by non-luminescent to bright luminescent sparite (Fig. 13E-F). Lithofacies L11 displays Fe oxide stained, bright luminescent laminar calcrete crusts with alveolar texture (Figs. 6, 10C).

Figure 14 shows the results of stable oxygen and carbon isotope analyses of bulk rocks, skeletal fragments, cement from all facies types, and calcrete crusts from lithofacies L11 (Table S1 Supplementary data). Most of the samples from lithofacies L1 to L14, with exception of L3 and L9, show $\delta^{18}O$ ranging from -3.5 to -6 ‰ and $\delta^{13}C$ varying from -3 to -10 ‰. The bulk analyses of lithofacies L3.1 and L3.2 display $\delta^{13}C$ and $\delta^{18}O$ values higher than most of the other lithofacies: $\delta^{18}O$ is around 1 ‰, whereas $\delta^{13}C$ varies from -0.1 ‰ to -0.4 ‰. In L3.2, $\delta^{18}O$ varies between -2.7 and -2.2 ‰, while $\delta^{13}C$ is about -1 ‰. The dolostone clasts from lithofacies L1 breccia have $\delta^{18}O$ between -2.7 ‰ and -3.8 ‰ and $\delta^{13}C$ values around -0.1 to -0.6 ‰, whereas the breccia interparticle matrix shows an isotopic signature similar to the other samples with $\delta^{18}O$ around -5 ‰ and $\delta^{13}C$ -4.5 ‰. Lithofacies L9 samples provided positive values for both $\delta^{13}C$ (about 1.3-1.4 ‰) and $\delta^{18}O$ (1.2 ‰). The calcrete crusts and bulk samples of lithofacies L11 record the most ^{13}C depleted $\delta^{13}C$ values, from -6.5 ‰ to -9.7 ‰.

5. Interpretation

5.1 Finale Ligure basin geometry

The Oligocene-Miocene carbonate-siliciclastic succession in the Finale Ligure area is interpreted as the gradual filling of an embayment (Finale Ligure basin), carved in the deformed and

eroded Alpine tectonic units following a marine transgression, as similarly proposed for Miocene flooded incised palaeo-valleys in Southern France (Reynaud et al., 2006, 2012; Reynaud and Jones, 2012; James et al., 2014).

The discontinuous lenses of massive dolostone breccia (L1) resulted from the erosion of the Triassic S. Pietro dei Monti Dolostone from the Alpine bedrock and might represent karstic breccia of undetermined age, predating the Oligocene-Miocene marine transgression and the flooding of the Finale Ligure basin. The lithofacies L2-L14 sedimentary succession reflects two main phases of marine sedimentation, separated by an angular unconformity (Fig. 8) documenting a tectonic event. The first depositional phase is represented by the stratigraphically lower lithofacies group (L2-L4) indicative of marine transgressive deposits non-conformably draping the Alpine bedrock. This lower lithofacies group records open marine facies, documenting rapid subsidence before the uplift responsible for the development of the overlying angular unconformity. The origin and age of this tectonic event can be inferred considering the regional evolution of the area, located at the junction between the Alps and Apennines orogens and the Tertiary Piedmont Basin (TPB). The TPB was affected by several tectonic phases during the Oligocene-early Miocene (Mosca et al., 2010). In particular, transpressional tectonics during the Aquitanian and early Burdigalian is reported in various studies on the TPB (Clari et al., 1995; Mutti et al., 1995; Mosca et al., 2010; Maino et al., 2013) and could have driven the uplift, tilting and erosion that generated the angular unconformity separating the lower lithofacies group L2-L4 from the overlying L5-L14 succession. After this tectonic event, the second depositional phase (intermediate L5-L7 and upper lithofacies L8-L14 groups) was characterized by absent to limited syn-depositional tectonics as in the TPB (Maino et al., 2013 report Langhian-Serravallian limited displacement of NE-SW oriented extensional and NW-trending contractional structures). The Finale Ligure Limestone succession does not record evidence of post-depositional deformations (Fig. 4), with the exception of a regional tilting toward the south. Therefore, it is assumed that the basal surface of the stratigraphic succession, comprising lithofacies L5 to L14 (terrigenous and calcareous deposits of the Finale Ligure Limestone), reflects

the original depositional surface of the Finale Ligure basin, only slightly tilted southward after deposition. The reconstruction of this basal surface represents an important constraint for the interpretation of the depositional processes that led to the filling of the Finale Ligure basin. The interpolation of a network of geological cross-sections extracted from the geological map (Fig. 4, 5) with the software package MOVE™ provided the 3D reconstruction of the morphology of the basin before the deposition of the Finale Ligure Limestone (Fig. 15). The absence of units overlying the Finale Ligure Limestone suggests that the present-day distribution may reflect the original extension of the Finale Ligure Limestone, providing good constraints for the reconstruction of the volume of the basin (Fig. 15). The Finale Ligure basin consisted of a sub-circular embayment (diameter approximately 5 km, nearly 35 km^2 wide) surrounded by the Alpine reliefs connected southward to the open sea through a narrow strait, bordered by a morphologic high in the southern part (Fig. 5, 15). In the SW Verezzi outcrops (Campi d'Orsi, Mt. Caprazoppa; Fig. 4) the evidence of meteoric diagenesis with laminar calcrete paleosols and abundant Fe oxides-hydroxides in lithofacies L11 may suggest a local subaerial exposure (Fig. 5, 15) of uncertain origin that could possibly be related to the NE-SW oriented extensional structures and NW-trending contractional structures, identified in the TPB by Maino et al. (2013) within Langhian-Serravallian deposits.

The 3D reconstruction of the Finale Ligure basin (Fig. 15) documents the existence of an embayment funnelling seaward through a narrow opening, with implications on the current pattern within the basin.

5.2 The Finale Ligure Limestone depositional environments

The depositional environment of the siliciclastic lithofacies L2-L4 cannot be exactly determined due to discontinuous outcrops. Based on sedimentary features, fossil content and the abundance of glaucony pellets (cf. Amorosi, 1997), lithofacies from the stratigraphically lower group L2, L3 and L4 are interpreted to represent the remnants of an eroded marine siliciclastic

shelf, subjected to tectonic uplift and erosion as suggested by the angular unconformity at the top of lithofacies L3 and L4 (Fig. 8). After this tilting, subsidence related to thrust loading, reported in late Burdigalian-Serravallian time (Carrapa et al., 2003), could be responsible for the accommodation available for the Finale Ligure Limestone succession, up to 150 m thick. The filling of the Finale Ligure embayment began with conglomerates and coarse litharenites with rare carbonate skeletal grains (intermediate lithofacies group L5, L6 and L7). These conglomerates and cross-bedded litharenites might represent coarse debris accumulated in rocky coastal settings along the northern and southern margins of the marine embayment limited by the Alpine bedrock, reworked in transgressive ravinement lags, as similar basal conglomerates were interpreted in various current-swept settings and marine flooded incised palaeo-valleys (cf. Longhitano, 2011; Chiarella et al., 2012; Chiarella and Longhitano, 2012; Reynaud and James, 2012; James et al., 2014; Longhitano et al., 2014, , 2021b). In the central part of the basin (Fig. 15), the L6 burrowed sandstone with glaucony might represent deposition in a deeper low-energy environment, below storm wave base (cf. Chiarella et al., 2012), overlying and lateral to the transgressive ravinement conglomerates, suggesting rapid creation of accommodation during transgression. Lithofacies L5-L7 are sharply overlain by the dominantly bioclastic, stratigraphically upper lithofacies group L8-L14 of the Finale Ligure Limestone that gradually filled the embayment during the Langhian-Serravallian, onlapping the Alpine bedrock and the underlying laterally discontinuous siliciclastic lithofacies L2-L4. Lithofacies L8 bedded litharenite and conglomerate with skeletal fragments records the onset of the skeletal carbonate production, but with a persisting siliciclastic input from the Alpine bedrock along the margins of the embayment. Lithofacies L9-L12 in the SW outcrop area of Verezzi, characterized by abundant micrite matrix, reworked skeletal fragments, common planktonic foraminifera and planar parallel and tabular cross-bedding (in L10 and L12), were deposited in an open marine, low to high-energy setting with intermittently current-swept seafloor. Planktonic foraminifera are almost exclusively observed in the SW Verezzi outcrops that are located on the southward seaward side of the bedrock morphologic high bordering the Finale Ligure embayment

towards the open sea (Figs. 5, 15). Lithofacies L12 occurs in both the Rocca di Perti-Mt. Cucco and Verezzi areas and shows a diverse skeletal composition (e.g., echinoderms, bivalves, bryozoans, barnacles, brachiopods, stylasterid and scleractinian corals, benthic foraminifera). Skeletal fragments might occur first lined by marine isopachous fibrous cement, and later embedded in micrite, suggesting that skeletal grains were partly cemented in high-energy, micrite-free environments, and then reworked and deposited in lower energy, micrite-rich settings. The presence of parallel or cross-stratified beds and the variable percentage of micrite matrix are indicative of intermittent bottom current hydrodynamic activity. The metre to decametre-scale tabular compound cross-bedding of lithofacies L12-L14 skeletal packstone to grainstone/rudstone indicates deposition in a current-swept high-energy seafloor, where metre-scale subaqueous dunes developed and migrated mostly southwards and from the margin to the centre of the embayment (Nembrini et al., 2017), while the Finale Ligure basin was filled by the locally produced skeletal carbonate sediment (Figs. 3-5, 15). Water depth of the Finale Ligure basin is difficult to determine but an estimate can be calculated using the subaqueous dune height assuming that it is reflected in the bedform thickness (cf. Yalin, 1964; Andrè et al., 2011; Reynaud et al. 2013; Telesca et al., 2020). The observed bedform heights vary from 1-5 m up to 10 m (Fig. 3, 11) suggesting water depth of 7-35 m up to 70 m. Baucon et al. (2020) focused their investigation on the *Bichordites* ichnofabric occurring in the Verezzi Mb. of the Finale Ligure Limestone suggesting it resulted from the activity of a community of irregular spatangoid infaunal echinoids bioturbating the subaqueous dunes identified by Nembrini et al. (2017). *Bichordites* ichnofacies suggests normal marine salinity, oxygenated bottom and water depths variable from 6-15 m to 50 m, but even up to 230 m (Baucon et al., 2020 and references therein). The alternation of bioturbation with unborrowed beds is indicative of fluctuating environmental conditions, shifting substrates, sedimentation rates and hydrodynamic energy, confirming the action of intermittent bottom currents.

Lithofacies character and sedimentary structures document that the seafloor of the Finale Ligure basin was swept by strong bottom currents, accelerated by the presence of the narrow strait

limiting the embayment connection to the open sea in the South (Figs. 5, 15). Morphologic constrictions promote the generation of strong currents, driven by tides and/or unidirectional marine currents, and the development of subaqueous dune fields (Dalrymple, 2010). According to Viana et al. (1998), relatively shallow water (50-300 m depth) siliciclastic and/or carbonate sands can develop bedforms in outer shelf and upper slope settings, resulting from the action of strong superficial geostrophic currents combined with storm wave-induced near-bottom orbital motion, tidal currents, and the rotatory effect of current eddies sweeping the seafloor. Anastas et al. (1997, 2006), in the upper Eocene-Miocene heterozoan carbonates of the Te Kuiti Group (North New Zealand), interpreted bioclastic (bryozoans, echinoderms, coralline algae, benthic foraminifera and bivalves) grainstone-packstone horizontally- and cross-bedded as deposited in a seaway in wave- and current-dominated settings, respectively. Current-dominated conditions prevailed when water depth was optimal (40-60 m) to allow flow acceleration through the seaway. The key factor affecting the strength of the tidal and oceanic currents was the cross-sectional area of the seaway (Anastas et al., 2006). In coastal embayments, tidal currents can increase in strength even in microtidal settings when the size and depth of the bay may cause a local amplification of the tidal wave (e.g., the Adriatic Sea, Central Mediterranean; Longhitano, 2011). In this type of current swept settings, either with siliciclastic or bioclastic carbonate sedimentation, the depositional models provided for continental shelves (shoreface to offshore zone; cf. Reading and Collinson, 1996) or carbonate ramps (inner, middle, outer ramp; cf. Burchette and Wright, 1992) have difficult applications (Dalrymple, 2010; James and Lukasik, 2010; Longhitano, 2013; James et al., 2014). Longhitano (2013) proposed a facies-based depositional model for tectonically-confined tidal straits. During marine transgressions, previous erosional topographic lows can turn into embayments and straits once inundated by marine waters; these embayments may be subjected to relevant tidal influence due to the coastal sheltering that constrains and amplifies the tidal current and minimize the wave effect (e.g., Yoshida et al., 2007; Longhitano, 2011; Chiarella and Longhitano, 2012; Chiarella et al., 2012; Longhitano et al., 2012ab, 2017). A similar mechanism

driving the increase of the current strength may be invoked for the Finale Ligure basin, where a narrow strait has been identified connecting the embayment with the open sea to the south (Fig. 15). The observed compound cross-bedding with multi-directional lamination might suggest that the Finale Ligure embayment was tidally-influenced, as similarly proposed for Miocene flooded palaeo-valleys in Southern France (Reynaud et al., 2006, 2012; Reynaud and Jones, 2012; James et al., 2014). Alternatively or in combination with the hypothesis of accelerated tidal currents, subaqueous dunes might be produced by episodic storm currents and storm surges as documented in some present-day microtidal settings. For example, during severe storms, in the Gulf of Gdańsk in the non tidal Baltic Sea (Cieślikiewicz et al., 2017) or along the coast of the Beaufort Sea (Canada), wind-induced sea-level rises are metre-scale, up to more than 2.4 m (Harper et al., 1988; Héquette and Hill, 1993). In the Canadian Beaufort Sea (Tibjak Beach), wind-induced bottom currents drive significant sediment remobilization as the threshold of sediment motion is exceeded by seaward-directed near-bottom currents associated with downwelling conditions with speeds up to 0.49 m/sec that can actively flow for more than 18 hours (Héquette and Hill, 1993). The geometry of the Finale Ligure embayment and severe storms in the Mediterranean region during the Miocene might have exerted a major control on the development of bottom currents able to mobilize skeletal and terrigenous sand dunes as those observed in the Finale Ligure Limestone, suggesting an origin of the bedforms not exclusively by tidal currents.

5.3 The Finale Ligure Limestone heterozoan carbonate factory

The Finale Ligure Limestone skeletal composition, dominated by heterotrophic suspension-feeding biota such as barnacles, bryozoans, echinoderms, molluscs and brachiopods, is an example of heterozoan carbonate association (cf. James, 1997; Mutti and Hallock, 2003; Halfar et al., 2004; Westphal et al., 2010). These heterozoan carbonates accumulated in a coastal embayment at warm temperate palaeo-latitudes (between 35°-40°N latitude according to Dercourt et al., 2000; de la Vara

and Meijer, 2016) during the mid-Miocene climatic optimum (approximately Burdigalian-Langhian) to the Serravallian transition to cooler conditions (Zachos et al., 2001; Billups and Scheiderich, 2010).

A dominant skeletal carbonate production of suspension-feeding heterotrophic organisms is indicative of abundant trophic resources (Hallock and Schlager, 1986; Mutti and Hallock, 2003; James and Lukasik, 2010). Barnacles, bryozoans and echinoids, which are abundant in the packstone/grainstone of the Finale Ligure Limestone, are most prolific in mesotrophic and eutrophic environments (James and Lukasik, 2010). Barnacles require hard substrates and are especially numerous in high-energy, high-latitude or high-nutrient environments, whereas molluscs and bryozoans are ubiquitous (James and Lukasik, 2010; Reynaud and James, 2012; Coletti et al., 2017, 2018a). The occurrence of glaucony and phosphate grains (Table 2) supports high nutrient levels (Pufhal, 2010; Reynaud and James, 2012; James et al., 2014) in the Finale Ligure basin, which must have derived from terrestrial run off and river input from the exposed Alpine reliefs surrounding the embayment as also suggested by (Brandano et al. (2015).

Coralline red algae dominated numerous Miocene carbonate depositional systems in the Mediterranean region, in particular from Burdigalian to early Tortonian times (Halfar and Mutti, 2005; Pomar and Hallock, 2007; Pomar et al., 2017; Coletti and Basso, 2020; Cornacchia et al., 2021 and references therein) but they are scarce to absent in the Finale Ligure Limestone. Coralline red algae are controlled by light, temperature, depth, salinity and nutrients (Adey and Macintyre, 1973; Coletti et al., 2018b). Coralline algae live in the whole photic zone, also near the photic limit and within a wide range of temperatures but water depth distribution varies at sub-family to genus level (Adey and Macintyre, 1973; Bosence, 1993; Basso, 1998; Lund et al., 2000; Braga and Aguirre, 2001; Coletti and Basso, 2020). In tropical waters coralline red algae are abundant in mesotrophic and oligophotic environments (Halfar and Mutti, 2005; Pomar and Hallock, 2007; James and Lukasik, 2010). For instance, in the Gulf of California, they dominate in the mesotrophic central area, whereas bryozoans and barnacles are most abundant in the eutrophic northern head of

the gulf (Halfar et al., 2004, 2006). Coralline red algae are reduced under eutrophic conditions because of reduced seafloor illumination due to unrestrained phytoplankton growth (James and Lukasik, 2010). Moreover, high concentrations of phosphate have an inhibitory effect on both growth and calcification rates of coralline algae (Björk et al., 1995). Lower Miocene carbonate systems in the Western Mediterranean were characterized by the dominance of coralline algae in moderate nutrient concentrations, while high nutrient concentrations produced carbonate factories with heterotrophic suspension-feeders such as bryozoans and barnacles (Coletti et al., 2017). Hence, the scarcity of red algae in the heterozoan carbonates of the Finale Ligure Limestone might be related to high levels of phosphate nutrients. These inferred environmental conditions might explain also the scarcity of mixotroph biota such as larger benthic foraminifera (cf. James and Lukasik, 2010). Light availability, fundamental for calcareous algae, might have been reduced due to high water depth and/or turbidity. Nevertheless, the reconstructed morphology of the Finale Ligure basin (Fig. 15) and the subaqueous dune size indicate an embayment a few tens of metres deep (inferred 7-70 m) excluding widespread aphotic seafloors. In addition, well-lit shallow-water settings would have been in any case available along the embayment margins. Scarce red algae fragments were identified in the SW outcrops of Verezzi (L11-L12), located towards the open sea, seaward of the morphologic threshold, where conditions preventing the red algae to thrive within the Finale Ligure embayment (probably high nutrients) were reduced in the more open marine setting, as demonstrated by the abundance of planktonic foraminifera in the SW outcrops of Verezzi.

Halimeda green algae were reported as important skeletal components of the Finale Ligure Limestone by Boni et al. (1968) and Bonci et al. (2019ab). Brandano et al. (2015) proposed that *Halimeda* played a predominant role as carbonate producer in the Finale Ligure Limestone, replacing seagrasses due to the high nutrient levels. In this study, the typical structures of Miocene halimedacean algae (cf. Braga et al., 1996; Martín et al., 1997; Flügel, 2004; Tournadour et al., 2020) were not recognized in the Finale Ligure Limestone. Although identification in thin section of former aragonitic skeletal grains, such as *Halimeda*, is problematic due to diagenetic

transformation, detailed petrographic analysis performed in this study indicates that most of the skeletal grains interpreted as *Halimeda* fragments in previous studies on the Finale Ligure Limestone are actually stylasterid corals. The discriminant features of stylasterid corals in the analysed thin sections (Fig. 12) are: (1) the typical dendritic or reticulate structures (Fig. 12B, G), resulting from the meshwork of tiny coenosteal canals, and (2) the tubular features, circular in transversal sections (Fig. 12B), ascribable to the gastropore and dactilopore tubes. Due to the poor preservation of the skeletons, it is difficult to recognise with certainty the tiny axial structures within the tubular features such as gastrostyles (Figs. 12 B, F) or cyclosystems (Fig. 12D). Skeletal components similar in thin sections to those presented in this study were described by Mastandrea et al. (2002) in the upper Miocene Mendicino Limestone (Southern Italy) and attributed to stylasterid corals.

Stylasterid corals presently thrive in a wide range of latitudes, from Antarctica to the Arctic Circle (Cairns, 2011). They live at various water depths from 0 m to 2200 m (Zibrowius and Cairns, 1992) although they are most common at 200-400 m in insular environments and 90% of the species occur deeper than 50 m (Cairns, 2007, 2011). Stylasteridae live in oligotrophic to eutrophic waters (Cairns, 1992) and typically in environments with intense water agitation both in shallow and deep waters (Cairns and Hoeksema, 1998; Häussermann and Försterra, 2007; Roberts et al., 2006; Salvati et al., 2010; Cooper et al., 2014; Roveta et al., 2019). Particularly interesting for the interpretation of the Finale Ligure Limestone is the frequent association of the stylasterid *Errina aspera* with the large barnacle *Pachylasma giganteum*, on substrates lashed by strong currents, both in the Early Pleistocene and in the present-day Messina Strait (Fredj and Giermann, 1982; Di Geronimo and Fredj, 1987; Zibrowius and Cairns, 1992; Salvati et al., 2010). *Errina aspera* is present in the Mediterranean Sea at depths of 90-220 m in the Messina Strait (Zibrowius and Cairns, 1992; Giacobbe et al., 2007) and along the Spanish coast of the Gibraltar Strait, from 61 m to around 440 m depth (Alvarez-Perez et al., 2005).

In the Finale Ligure Limestone, stylasterid corals form centimetre-scale clusters with solitary or small colonies of scleractinian corals classified as boundstone in L14. Due their poor preservation, scleractinian corals could be only tentatively identified at family level as Dendrophylliidae (Fig. 12A) and Caryophylliidae (Fig. 12B). Both scleractinian and stylasterid corals probably lived on hard rocky substrates around the margins of the basin or settled their larvae on siliciclastic debris or skeletal fragments. The abundance of heterotrophic suspension feeders, the scarcity or absence of autotrophic (red coralline and green algae) and mixotrophic (larger benthic foraminifera such as *Amphistegina*) biota in the whole Finale Ligure Limestone succession might point to scleractinian corals lacking photosymbionts, able to thrive in high-energy and high-nutrient settings not limited by bathymetry, trophic resources and water temperature. The early-middle Miocene is considered a flourishing time interval for Mediterranean azooxanthellate corals (Vertino et al., 2014). Brandano et al. (2015) indicated the presence of azooxanthellate corals in the bivalve floatstone facies of the Finale Ligure Limestone. Azooxanthellate corals were also described in cross-bedded bioclastic limestone associated with barnacles, bryozoans and red algae in lower Miocene heterozoan carbonates in flooded incised palaeo-valleys in southern France (Reynaud and James, 2012; James et al., 2014). In the upper Tortonian-lower Messinian Mendicino Limestone, Mastandrea et al. (2002) reported that stylasterid corals formed coral banks in deep-water, approximately at 100 m, associated with azooxanthellate scleractinians (*Oculina* and *Dendrophyllia*), bryozoans, echinoids, benthic foraminifera, gastropods, bivalves, planktonic foraminifera in the micrite matrix, and lacked calcareous algae. The Mendicino Limestone coral banks were adjacent to bioclastic subaqueous dunes with barnacle fragments and were interpreted as developed in meso-eutrophic conditions, in the aphotic zone, on seafloors affected by deep currents, siliciclastic sediment and abundant nutrient (Mastandrea et al., 2002). Barrier et al. (1991) described a high diversity coral fauna in the Messinian deposits of the Betic Cordilleras (Brèche Rouge de Carboneras, SE Spain), including calcified sponges, stylasterids, scleractinians (mostly Dendrophyllidae), gorgonians, stalked crinoids, gastropods, brachiopods and barnacles. This

association developed on a bathyal hardground on olistoliths of volcanic rocks at depths of several hundred metres in aphotic conditions similarly to present-day coral associations on hard substrates in the upper bathyal bathymetric zone offshore New Caledonia (Brachert et al., 2001; Krautworst and Brachert, 2003).

The Finale Ligure Limestone skeletal carbonates could represent a transitional heterozoan-photozoan carbonate association or warm temperate heterozoan carbonates (cf. Halfar et al., 2006; James and Lukasik, 2010) if the scleractinian corals were zooxanthellate. Nevertheless, the results of this study support the interpretation that the Finale Ligure Limestone represents an example of heterozoan carbonates dominated by barnacles, bryozoans and echinoderms associated with stylasterid corals and, possibly azooxanthellate, scleractinian corals, influenced by high nutrient levels and strong bottom currents in a confined embayment.

5.4 Diagenesis and stable isotope of Finale Ligure heterozoan carbonates

Diagenetic investigation and stable isotope data contributed to constraining the post-depositional history of the studied succession. The presence of concavo-convex grain contacts, fracturing and rare stylolites documents mechanical compaction and pressure solution preceding calcite cementation (Bathurst, 1987; Tucker and Wright, 1990). Pressure solution can occur at relative low pressure (Tada and Siever, 1989); in fact, depths of initial appearance of stylolites in limestones are reported as shallow as 90 m (Schlanger et al., 1964). All the lithofacies from L2 to L14 show evidence of dissolution and cement precipitation postdating mechanical compaction, such as non-luminescent scalenohedral and blocky cements related to meteoric or shallow burial diagenesis also filling bio-mouldic and vuggy porosity. Lithofacies L12-L14 display limited early marine cementation preceding compaction, represented by isopachous rims of fibrous cement enveloping bioclasts, followed by meteoric scalenohedral to blocky calcite. In lithofacies L12 packstone, the skeletal fragments lined by early marine cement rims were reworked by currents and

transported in low-energy marine environments, as documented by micrite filling the interparticle porosity. Metastable carbonates (aragonite, high Mg-calcite) are generally dissolved or replaced by calcite (Tucker and Wright, 1990; Brachert and Dullo, 2000). In lithofacies L12-L14, aragonite bioclasts, such as molluscs, stylasterid and scleractinian corals, but also calcite bioclasts (barnacles, benthic foraminifera) occur as dissolved biomoulds or replaced by low Mg calcite spar. The carbonate source for the pervasive meteoric and shallow burial cementation could be genetically related to the dissolution of these skeletal fragments as similarly suggested for the Oligocene-Miocene heterozoan carbonate successions in Sicily and Malta by Knoerich and Mutti (2003, 2006ab). The low-Mg calcite biota, such as barnacles, were in some cases replaced by luminescent sparite. These skeletal components were probably altered in contact with phreatic meteoric or shallow burial reducing fluids that allowed Mn^{2+} to be incorporated in the calcite crystals (Machel, 1985).

Expected oxygen and carbon stable isotope values for lower-middle Miocene open marine carbonates should be 1.5-2 ‰ for $\delta^{18}O$ and 1-2 ‰ for $\delta^{13}C$ (Zachos et al., 2001). The measured $\delta^{18}O$ and $\delta^{13}C$ values deviate from the expected marine signature, except for lithofacies L3 and L9, suggesting diagenetic alteration from meteoric water, as also inferred from petrographic analysis (e.g., scalenohedral cement), which tends to shift the rock geochemical signature to lower $\delta^{13}C$ and $\delta^{18}O$ values (Tucker and Wright, 1990; Swart, 2015). The calcrete crusts of lithofacies L11 in the SW outcrops of Verezzi are strongly depleted in ^{13}C, confirming the influence of meteoric fluids enriched in ^{12}C derived from the soil organic matter. The L1 massive dolostone breccias have a sedimentary and diagenetic history different from the other facies. The dolostone was affected by burial diagenesis as demonstrated by the clast $\delta^{13}C$ and $\delta^{18}O$ values, whereas the isotopic signature of the interparticle matrix reflects a meteoric diagenetic environment supporting the karstic breccia interpretation.

Overall, the diagenetic features and stable oxygen and carbon isotope values of the analysed lithofacies are indicative of limited marine diagenesis and predominance of meteoric and shallow

burial diagenesis as observed in other heterozoan carbonate case studies (James et al., 2005; Knoerich and Mutti, 2006ab; Caron and Nelson, 2009).

6. Discussion – The Finale Ligure Limestone a Miocene example of heterozoan carbonates in confined embayment

Miocene carbonate successions in the Mediterranean region display a wide spectrum of carbonate factories (photozoan vs. heterozoan), depositional system geometry (high-relief vs. ramps), facies character and architecture under the influence of palaeolatitude, palaeoclimate, nutrient levels, hydrodynamic energy, substrate type, relative sea level and tectonic setting (Pomar and Hallock, 2007; Pomar et al., 2004, 2012, 2017; Brandano et al., 2016, 2017ab; Cornacchia et al., 2021). Lower Miocene Mediterranean carbonate factories were controlled by nutrient concentrations: coralline algae were dominant in moderate nutrient levels whereas heterotrophic suspension-feeders, such as bryozoans, in high nutrient conditions; euphotic-zone carbonate producers, which thrive in tropical photozoan associations, were restricted to areas with low nutrient concentrations (Coletti et al., 2017 and references therein). Within the broad range of Miocene carbonate systems, the lower-middle Miocene succession of the Finale Ligure Limestone represents a mixed skeletal heterozoan carbonate and siliciclastic system accumulated in a marine embayment with high nutrient levels. High-nutrient conditions were proposed by Brandano et al. (2015) who defined the Finale Ligure depositional system as a progradational coastal wedge. This study shows that the Finale Ligure basin was a confined embayment swept by strong currents forming metre-scale subaqueous dunes made of different ratios of skeletal (intrabasinal) and terrigenous (extrabasinal) grains sourced from the surrounding emerged Alpine reliefs. In this setting, carbonate sand bedforms were driven by the amplification of currents due to the presence of a narrow strait connecting the Finale Ligure embayment with the open sea to the South. Hence, the Finale Ligure

Limestone represents an example of heterozoan carbonate system fitting with the seaway facies model (cf. Dalrymple, 2010; James and Lukasik, 2010; Michel et al., 2018).

Despite the differences with the Miocene Finale Ligure embayment in terms of size, water depth, tidal setting and sediment types, present-day examples of sedimentation in seaways, straits and embayments where subaqueous dunes develop due to accelerated tide-, wind-induced and oceanic currents provide useful insights on such depositional settings. Some well-studied examples are: the Torres Strait (Gulf of Papua; Hemer et al., 2004), Bawihka Channel (Nicaragua Rise; Hine et al., 1994), the Mouth of San Francisco Bay (California; Barnard et al., 2006; Longhitano, 2013), the English Channel (Reynaud et al., 2003) and the Messina Strait (between Sicily and Calabria regions, southern Italy; Santoro et al., 2002; Longhitano, 2013, 2018ab; Longhitano et al., 2021a). In these case studies, sediment composition varies from siliciclastic to carbonate to mixed carbonate-siliciclastic according to the latitude, oceanography and nutrient levels. Terrigenous sediment can derive from rivers, fan deltas, or marginal cliff collapses but in many modern and ancient seaways *in situ* bioclastic carbonate production is often the dominant sediment source (Longhitano, 2013). At the Mouth of San Francisco Bay, 10 m high subaqueous dunes develop in the tidal inlet that connects San Francisco Bay to the Pacific Ocean at water depth of 30-106 m, due to the complex interaction of waves and tidal currents in a narrow seaway (Barnard et al., 2006; Hanes and Barnard, 2007; Barnard et al., 2013). The skeletal composition of the present-day Messina Strait subaqueous dunes shows similarities with the Finale Ligure Limestone, even if the morphology and the bathymetry of the basin are markedly different. Giacobbe et al. (2007) recorded the presence of the stylasterid coral *Errina aspera* in the present-day Sicilian side of the strait, located on rocky bottoms at depths of 90-220 m. The twilight zone of the Messina Strait is characterized by a rocky substrate, lashed by strong currents that prevent the deposition of fine sediment, colonized by a benthic community where *Errina aspera* covers from 1.3 to 56 % per area (Salvati et al., 2010). The common presence of stylasterid and azooxanthellate corals is also recorded in the Messina Strait Pleistocene deposits (Vertino, 2003; Vertino et al., 2014).

A present-day example comparable, in terms of sedimentary features and skeletal composition, with the Finale Ligure basin is the Spencer Gulf in South Australia (James et al., 2014; O'Connell et al., 2016), a large (22,000 km^2), shallow (< 60 m deep) embayment with heterozoan carbonate sedimentation. The Spencer Gulf is dominated by strong bottom currents, with maximum speed on seafloor at about 20 m of water depth (O'Connell et al., 2016), in this case triggered by a major inverse estuarine circulation, creating seaward directed subaqueous dunes. In terms of skeletal sediment composition, barnacles, bivalves, bryozoans and echinoids occur in the Spencer Gulf similarly to the Finale Ligure Limestone, whereas coralline red algae, abundant in the Spencer Gulf, are rare to absent in the Finale Ligure Limestone lithofacies, which instead is enriched in scleractinian and stylasterid corals. Another difference is that the Spencer Gulf is characterized by growth of seagrasses meadows, which seem to lack in the Finale Ligure embayment as remarked by Brandano et al. (2015), who attributed the absence of seagrasses in the Finale Ligure Limestone to high nutrient levels.

In the geological record, numerous case studies of current-swept seaways and embayments have been identified, in particular from Miocene and Pliocene-Pleistocene successions in the Mediterranean realm. Mixed carbonate siliciclastic lithoclastic-bioclastic subaqueous dunes, attributed to amplified tidal currents, were identified in Pliocene-Pleistocene and Miocene coastal embayments and straits in Southern Italy, between the regions of Basilicata, Calabria and Sicily (Colella and D'Alessandro, 1988; Longhitano et al., 2010; Longhitano, 2011; Chiarella and Longhitano, 2012; Chiarella et al., 2012; Longhitano et al., 2012ab; Longhitano, 2013; Chiarella et al., 2016; Rossi et al., 2017; Longhitano, 2018b; Chiarella et al., 2019; Slootman et al., 2019), Pliocene Carboneras embayment (Spain, Martín et al., 2004); tidal dominated seaways between the Atlantic Ocean and Mediterranean Sea in the Miocene of the Betic Cordillera (Soria et al., 1999; Martín et al., 2001; Betzler et al., 2006; Braga et al., 2010; Martín et al., 2009, 2014); Miocene tide-dominated seaways in the central Sardinian Graben System (Longhitano et al., 2017; Telesca et al., 2020), lower-middle Miocene Bonifacio Basin evolving from an embayment to a strait connecting

the Western Mediterranean and the East Corsica Basin, where the tidal flow was accelerated due to the constriction of the marine strait (South Corsica, France; Ferrandini et al., 2002; André et al., 2011; Reynaud et al., 2013; Tomassetti and Brandano, 2013; Tomassetti et al., 2013), lower-middle Miocene Saint-Florent Basin (N Corsica, France, Ferrandini et al., 1998; Brandano and Ronca, 2014), Miocene tidal current-dominated flooded incised paleo-valleys in SE France (Reynaud et al., 2006; Reynaud and James, 2012; James et al., 2014; Coletti et al., 2017, 2018ab). The proposed tidal origin of the currents characterising these basins suggests that in the microtidal Neogene Mediterranean region amplification of tidal currents in seaways, straits and embayments was a common phenomenon in a complex paleogeographic, tectonically-active setting. According to Longhitano (2011), microtidal confined coastal areas, as in the Mediterranean Sea, are characterized by unidirectional, longshore to offshore directed currents that are responsible for the development of cross-bedding lacking mud. The signal of the dominant waves is mitigated by the engulfed morphologies and short-term tidal oscillations represent the dominant hydrodynamics in these basins where tidal amplification results from the basin geomorphological and hydrodynamic characteristics (Longhitano, 2011; Chiarella and Longhitano, 2012).

The depositional architecture and carbonate lithofacies association of the Finale Ligure Limestone show similarities and differences with other Miocene heterozoan carbonate successions in confined settings in the Mediterranean area. Similarities are related to the presence of metre-scale subaqueous dunes and abundance of heterozoan association skeletal grains, accumulated on seafloors swept by amplified tidal and storm currents. The Finale Ligure Limestone differs from other Mediterranean Miocene successions for some specific characters (e.g.; scarcity of red algae and larger benthic foraminifera, abundance of barnacles, scleractinian and stylasterid corals) indicative of depth- and light-independent skeletal biota dominating due to local conditions, likely represented by the availability of hard substrates and high nutrient levels in coastal environment, where the basin morphology favoured the acceleration of marine currents.

7. Conclusions

The Miocene Finale Ligure Limestone (Finale Ligure, NW Italy) represents a mixed carbonate-siliciclastic succession accumulated in a confined embayment connected through a strait with the open sea, favouring the development of strong currents. A marine transgression over previously exposed and eroded Alpine tectonic units created the suitable environmental conditions for the onset of heterozoan carbonate accumulation mixed with siliciclastic detrital sediment sourced from the surrounding Alpine bedrock.

The succession is composed of 14 lithofacies types (L1-L14). Lithofacies L1 is a residual karstic breccia reworking the Alpine bedrock, overlain by transgressive marine deposits belonging to two sedimentary successions separated by an angular unconformity. The stratigraphically lower, Oligocene to lower Miocene, marine terrigenous lithofacies L2-L4 represent the preserved remnants of eroded marine shelf deposits and include marlstone and wackestone with planktonic foraminifera, siltstones, and litharenites with glaucony, tilted and eroded after deposition. An angular unconformity, related to a regional tectonic phase, separates L2-L4 from the overlying siliciclastic lithofacies L5-L7 litharenites and conglomerates that are sharply overlain by the Finale Ligure Limestone skeletal carbonate-rich lithofacies (L8-L14). The onset of heterozoan carbonate production is characterized by cross-bedded packstone to grainstone/rudstone with barnacles, bivalves, echinoderms, bryozoans, scleractinian and stylasterid corals, deposited in a high-energy, current-swept setting. Seaward migrating, metre-scale subaqueous dunes developed in the Finale Ligure basin due to accelerated currents (possibly originated by tides, storms and/or winds) within the confined embayment surrounded by the Alpine bedrock connected towards the open sea through a strait.

Compared to other lower-middle Miocene carbonate systems in the Mediterranean region, the Finale Ligure Limestone skeletal composition is a heterozoan depth- and light-independent biotic association as suggested by the absence of green algae, the scarce presence of red algae and

larger benthic foraminifera (*Amphistegina*), and the abundance of stylasterid and, possibly azooxanthellate, scleractinian corals. This study demonstrates the important contribution of stylasterid corals to carbonate production in the Finale Ligure Limestone, reducing the role assigned to *Halimeda* by previous authors.

The specific carbonate-producing skeletal association with respect to other Miocene carbonate successions of the Miocene Mediterranean region and the cross-stratified sedimentary features of the Finale Ligure Limestone can be ascribed to the confined morphology of the embayment, with facies character and composition controlled by hydrodynamic energy, availability of hard substrates and high nutrient levels in a coastal environment.

Data availability

Data supporting this study are presented in this manuscript; additional data will be made available upon request to the authors.

Declaration of competing interest

The authors declare that they have no known competing financial interests or personal relationships that could have appeared to influence the work reported in this paper.

Acknowledgments

The authors would like also to thank Curzio Malinverno (University of Milan) for thin-section preparation, Elena Ferrari (University of Milan) for stable isotope analyses and Stefano Fiorani for help in the field and in preparation of the 3D Move model. Prof. Maria Rose Petrizzo (University of Milan) was instrumental for sample preparation and determination of the planktonic and benthic foraminifera in the marly deposits. The reviewer Domenico Chiarella, an anonymous

reviewer and Editor Brian Jones are thanked for their valuable comments improving this manuscript.

Appendix A. Supplementary data

Supplementary data to this article can be found online at https://doi.

References

Adey, W.H., Macintyre, I.G., 1973. Crustose Coralline Algae: A Re-evaluation in the Geological Sciences. Geological Society of America Bulletin 84, 883-904.

Alvarez, V., 1976. A former continuation of the Alps. Geological Society of America Bulletin 87, 891-896.

Alvarez-Pérez, G., Busquets, P., De Mol, B., Sandoval, N.G., Canals, M., Casamor, J.L., 2005. Deep-water coral occurrences in the Strait of Gibraltar. In Freiwald A. and Roberts J.M. (eds) Cold-water corals and ecosystems. Berlin, Heidelberg: Springer-Verlag, pp. 207–221.

Amorosi, A., 1997. Detecting compositional, spatial, and temporal attributes of glaucony: a tool for provenance research. Sedimentary Geology 109, 135-153.

Anastas, A.S., Dalrymple, R.W., James, N.P., Nelson, C.S., 1997. Cross-stratified calcarenites from New Zealand: subaqueous dunes in a cool-water, Oligo-Miocene seaway. Sedimentology 44, 869-891.

Anastas, A.S., Darlymple, R.W., James, N.P., Nelson, C.S., 2006. Lithofacies and dynamics of a cool-water carbonate seaway: mid-Tertiary, Te-Kuiti Group, New Zealand. In: Pedley, H.M., Carannante, G. (Eds.), Cool-Water Carbonates: Depositional Systems and Palaeoenvironmental Controls. Geological Society London, Special Publication 255, 245-268.

André, J.P., Barthet, Y., Ferrandini, M., Ferrandini, J., Reynaud, J.Y., Tessier, B., 2011. The Bonifacio Formation (Miocene of Corsica): transition from a wave- to tide-dominated coastal system in mixed carbonate-siliciclastic setting. Bulletin de la Société géologique de France 182, 221-230.

Andreucci, S., Pistis, M., Funedda, A., Loi, A., 2017. Semi-isolated, flat-topped carbonate platform (Oligo-Miocene, Sardinia, Italy): Sedimentary architecture and processes. Sedimentary Geology 361, 64-81.

Arobba, D., Bonci, M.C., De Pascale, A., Piazza, M.,2019. Un atlante di macrofossili della Pietra di Finale. In: Murialdo, G., Cabella, R., Arobba, D. (eds), Pietra di Finale. Una risorsa naturale e storica del Ponente ligure. Istituto Internazionale di Studi Liguri ONLUS - Bordighera (IM), 6175.

Barnard, P.L., Hanes, D.M., Rubin, D.M., Kvitek, R.G., 2006. Giant sand waves at the mouth of San Francisco Bay. Eos 87 (29), 285-289.

Barnard, P.L., Erikson, L.H., Elias, E.P.L., Dartnell, P., 2013. Sediment transport patterns in the San Francisco Bay Coastal System from cross-validation of bedform asymmetry and modeled residual flux. Marine Geology 345, 72-95.

Barrier, P., Zibrowius, H., Lozouet, P., Montenat, C., d'Estevou, P. O., Serrano, F., Soudet, H.J., 1991. Une faune de fond dur du bathyal supérieur dans le Miocène terminal des cordillères bétiques (Carboneras, SE Espagne). Mésoge 51, 3-13.

Basso, D., 1998. Deep rhodolith distribution in the Pontian Islands, Italy: a model for the paleoecology of a temperate sea. Palaeogeography, Palaeoclimatology, Palaeoecology 137, 173-187.

Bathurst, R.G.C., 1987. Diagenetically enhanced bedding in argillaceous platform limestones: stratified cementation and selective compaction. Sedimentology 34, 749-778.

Baucon, A., Piazza, M., Cabella, R., Bonci, M.C., Capponi, L., de Carvalho, C.N., Briguglio, A., 2020. Buildings that 'Speak': Ichnological Geoheritage in 1930s Buildings in Piazza della Vittoria (Genova, Italy). Geoheritage, 12, 70, 1-22. https://doi.org/10.1007/s12371-020-00496-x.

Benisek, M.F., Betzler, C., Marcano, G., Mutti, M., 2009. Coralline-algal assemblages of Burdigalian platform slope: implications for carbonate platform reconstruction (northern Sardinia, western Mediterranean Sea). Facies 55, 375-386.

Betzler, C., Brachert, T.C., Nebelsick, J., 1997. The warm temperate carbonate province: a review of the facies, zonations, and delimitations. Courier Forschungsinstitut Senckenberg 201, 83-99.

Betzler, C., Braga, J.C., Martín, J.M., Sánchez-Almazo, I.M., Lindhorst, S., 2006. Closure of a seaway: stratigraphic record and facies (Guadix Basin, Southern Spain). International Journal of Earth Sciences (Geologische Rundschau) 95, 903-910.

Billups, K., Scheiderich, K., 2010. A synthesis of Oligocene through Miocene deep sea temperatures as inferred by Mg/Ca ratios. In: Mutti, M., Piller, W.E., Betzler, C. (Eds.), Carbonate system during the Oligocene-Miocene Climatic Transition. IAS International Association of Sedimentologist, Special Publication 42, pp. 1–16.

Björk, M., Mohammed, S.M., Björklund, M., Semesi, A., 1995. Coralline algae, important coral-reef builders threatened by pollution. Ambio 24, 502-505.

Bonci, M.C., Cabella, R., Faccini, F., Firpo, M., Mandarino, A., Piazza, M., 2019a. Geologia, paleontologia e geomorfologia della Pietra di Finale. In: Murialdo, G., Cabella, R., Arobba, D. (eds), Pietra di Finale. Una risorsa naturale e storica del Ponente ligure. Istituto Internazionale di Studi Liguri ONLUS - Bordighera (IM), 11–32.

Bonci, M.C., Cabella, R., Piazza, M., Tedeschi, F., 2019b. Le “facies” della Pietra di Finale: un atlante. In: Murialdo, G., Cabella, R., Arobba, D. (eds), Pietra di Finale. Una risorsa naturale e storica del Ponente ligure. Istituto Internazionale di Studi Liguri ONLUS - Bordighera (IM), 45-60.

Boni, P., Mosna, S., Vanossi, M., 1968. La Pietra di Finale (Liguria Occidentale). Atti dell’Istituto Geologico dell’Università di Pavia 18, 102-150.

Boni, A., Cerro, A., Gianotti, R., Vanossi, M., 1971. Note Illustrative della Carta Geologica d’Italia alla scala 1:100.000, foglio 92-93 Albenga-Savona. Servizio Geologico d’Italia, 89-93.

Bonino, E., 2019. La nascita della Pietra di Finale e una ricostruzione ideale del mare miocenico. In: Murialdo, G., Cabella, R., Arobba, D. (eds), Pietra di Finale. Una risorsa naturale e

storica del Ponente ligure. Istituto Internazionale di Studi Liguri ONLUS - Bordighera (IM), 77-83.

Bosence, D.W.J., 1983. The occurrence and ecology of recent rhodoliths – a review. In: Peryt T. M. (Ed.), Coated Grains. Springer-Verlag, Berlin, pp. 217-224.

Brachert, T.C., Dullo, W.C., 2000. Shallow burial diagenesis of skeletal carbonates: selective loss of aragonite shell material (Miocene to Recent, Queensland Plateau and Queensland Trough, NE Australia) – implications for shallow cool-water carbonates. Sedimentary Geology 136, 169-187.

Brachert, T.C., Hultzsch, N., Knoerich, A.C., Krautworst, U.M., Stuckrad, O.M., 2001. Climatic signatures in shallow-water carbonates: high-resolution stratigraphic markers in structurally controlled carbonate buildups (Late Miocene, southern Spain). Palaeogeography, Palaeoclimatology, Palaeoecology 175, 211-237.

Braga, J.C., Aguirre, J., 2001. Coralline algal assemblages in upper Neogene reef and temperate carbonates in Southern Spain. Palaeogeography, Palaeoclimatology, Palaeoecology 175, 27-41.

Braga, J.C., Martín, J.M., Riding, R., 1996. Internal structure of segment reefs: *Halimeda* algal mounds in the Mediterranean Miocene. Geology 24, 35-38.

Braga, J.C., Martín, J.M., Aguirre, J., Baird, C.D., Grunnaleite, I., Jensen, N.B., Puga-Bernabéu, A., Sælen, G., Talbot, M.R., 2010. Middle Miocene (Serravallian) temperate carbonates in a seaway connecting the Atlantic Ocean and the Mediterranean Sea (North Betic Strait, S Spain). Sedimentary Geology 225, 19-33.

Brandano, M., Corda, L., 2002. Nutrients, sea level and tectonics: constrains for the facies architecture of a Miocene carbonate ramp in central Italy. Terra Nova 14, 257-262.

Brandano, M., Ronca, S., 2014. Depositional processes of the mixed carbonate-siliciclastic rhodolith beds of the Miocene Saint-Florent Basin, northern Corsica. Facies 60, 73-90.

Brandano, M., Tomassetti, L., Frezza, V., 2015. *Halimeda* dominance in the coastal wedge of Pietra di Finale (Ligurian Alps, Italy): The role of trophic conditions. Sedimentary Geology 320, 30-37. https://doi.org/10.1016/j.sedgeo.(2015).02.001.

Brandano, M., Cornacchia, I., Raffi, I., Tomassetti, L., 2016. The Oligocene-Miocene stratigraphic evolution of the Majella carbonate platform (Central Apennines, Italy). Sedimentary Geology 333, 1-14.

Brandano, M., Cornacchia, I., Tomassetti, L., 2017a. Global versus regional influence on the carbonate factories of Oligo-Miocene carbonate platforms in the Mediterranean area. Marine and Petroleum Geology 87, 188-202.

Brandano, M., Cornacchia, I., Raffi, I., Tomassetti, L., Agostini, S., 2017b. The Monterey Event within the Central Mediterranean area: The shallow-water record. Sedimentology 64, 286-310.

Burchette, T.P., Wright, V.P., 1992. Carbonate ramp depositional systems. Sedimentary Geology 79, 3-57.

Cairns, S.D., 1992. Worldwide Distribution of the Stylasteridae (Cnidaria: Hydrozoa). In: Bouillon, V., Boero, F., Cicogna, F., Gili, J.M., Hughes, R.G. (Eds), Aspects of Hydrozoan Biology, SCI. MAR. 56 (2-3), 125-130.

Cairns, S.D., 2011. Global diversity of the stylasteridae (Cnidaria: Hydrozoa: Athecatae). PloS one, 6(7), e21670.

Cairns, S.D., Hoeksema, B.W., 1998. *Distichopora vervoorti*, a new shallow-water stylasterid coral (Cnidaria: Hydrozoa: Stylasteridae) from Bali, Indonesia. Zoologische Verhandelingen, 323(24), 311-318.

Cairns, S.D., 2007. Deep-water corals: an overview with special reference to diversity and distribution of deep-water scleractinian corals. Bulletin of Marine Science 81, 311-322.

Carannante, G., Esteban, M., Milliman, J.D., Simone, L., 1988. Carbonate lithofacies as paleolatitude indicators: problems and limitations. Sedimentary Geology 60, 333-346.

Carminati E., Doglioni, C., 2005. Mediterranean tectonics. Encyclopedia of Geology 2, 135-146.

Carminati, E., Wortel, M.J.R., Meijer, P.T., Sabadini, R., 1998. The two-stage opening of the western-central Mediterranean basins: a forward modeling test to a new evolutionary model. Earth and Planetary Science Letters 160, 667-679.

Caron, V., Nelson, C.S., 2009. Diversity of neomorphic fabrics in New Zealand Plio-Pleistocene cool-water limestones: insights into aragonite alteration pathways and controls. Journal of Sedimentary Research 79, 226-246.

Carrapa, B., Bertotti, G., Krijgsman, W., 2003. Subsidence, stress regime and rotation(s) of a tectonically active sedimentary basin within the western Alpine Orogen: the Tertiary Piedmont Basin (Alpine domain, NW Italy). In: McCann, T., Saintot, A. (Eds.), Tracing tectonic deformation using the sedimentary record. Geological Society, London, Special Publication 208, pp. 205-227.

Chiarella, D., Longhitano, S.G., 2012. Distinguishing depositional environments in shallow-water mixed, bio-siliciclastic deposits on the basis of the degree of heterolithic segregation (Gelasian, southern Italy). Journal of Sedimentary Research 82, 969-990.

Chiarella, D., Longhitano, S.G., Sabato, L., Tropeano, M., 2012. Sedimentology and hydrodynamics of mixed (siliciclastic-bioclastic) shallow-marine deposits of Acerenza (Pliocene, Southern Apennines, Italy). Italian Journal of Geosciences, 131, 136-151.

Chiarella, D., Longhitano, S.G., Tropeano, M., 2017. Types of mixing and heterogeneities in siliciclastic-carbonate sediments. Marine and Petroleum Geology 88, 617-627.

Chiarella, D., Longhitano, S.G., Tropeano, M., 2019. Different stacking patterns along an active fold-and-thrust belt - Acerenza Bay, Southern Apennines (Italy). Geology 47, 139-142. https://doi.org/10.1130/G45628.1.

Chiarella, D., Moretti, M., Longhitano, S.G., Muto, F., 2016. Deformed cross-stratified deposits in the Early Pleistocene tidally-dominated Catanzaro strait-fill succession, Calabrian Arc

(Southern Italy): Triggering mechanisms and environmental significance. Sedimentary Geology, 344, 277-289.

Cieślikiewicz, W., Dudkowska, A., Gic-Grusza, G., & Jędrasik, J., 2017. Extreme bottom velocities induced by wind wave and currents in the Gulf of Gdańsk. Ocean Dynamics, 67, 1461-1480.

Clari, P., Dela Pierre, F., Novaretti, A., Timpanelli, M. 1995. Late Oligocene–Miocene sedimentary evolution of the critical Alps/Apennines junction: the Monferrato area, Northwestern Italy. Terra Nova 7, 144-152.

Colella, A., D'Alessandro, A., 1988. Sand waves, *Echinocardium* traces and their bathyal depositional setting (Monte Torre Palaeostrait, Plio-Pleistocene, southern Italy). Sedimentology 35, 219-237.

Coletti, G., Bosio, G., Collareta, A., Buckeridge, J., Consani, S., El Kateb, A., 2018a. Palaeoenvironmental analysis of the Miocene barnacle facies: case studies from Europe and South America. Geologica Carpathica 69, 573-592.

Coletti, G., Basso, D., 2020. Coralline algae as depth indicators in the Miocene carbonates of the Eratosthenes Seamount (ODP Leg 160, Hole 966F). Geobios 60, 29-46.

Coletti, G., Basso, D., Corselli, C., 2018b. Coralline algae as depth indicators in the Sommières Basin (early Miocene, Southern France). Geobios 511, 15-30.

Coletti, G., El Kateb, A., Basso, D., Cavallo, A., Spezzaferri S., 2017. Nutrient influence on fossil carbonate factories: evidence from SEDEX extractions on Burdigalian limestones (Miocene, NW Italy and S France). Palaeogeography, Palaeoclimatology, Palaeoecology 475, 80-92.

Cornacchia, I., Agostini, S., Brandano, M., 2018. Miocene oceanographic evolution based on the Sr and Nd isotope record of the Central Mediterranean. Paleoceanography and Paleoclimatology 33, 31-47.

Cornacchia, I., Brandano, M., Agostini, S., 2021. Miocene paleoceanographic evolution of the Mediterranean area and carbonate production changes: A review. Earth-Science Reviews 221, 103785.

Dallagiovanna, G., Gaggero, L., Seno, S., Felletti, F., Mosca, P., Decarlis, A., Pellegrini, L., Poggi, F., Bottero, D., Mancin, N., Lupi, C., Bonini, L., Lualdi, A., Maino, M., Toscani, G., 2011. Note Illustrative della Carta Geologica d'Italia alla scala 1:50.000, foglio 228 Cairo Montenotte. ISPRA - Regione Liguria, Litografia Artistica Cartografica s.r.l. 156 p.

Dalrymple, R.W., 2010. Tidal depositional systems. In: James, N.P., Dalrymple, R.W. (Eds.), Facies Models 4. Geological Association of Canada, GEOtext 6, St John's, Newfoundland, pp. 201–231.

de la Vara, A., Meijer, P., 2016. Response of Mediterranean circulation to Miocene shoaling and closure of the Indian Gateway: a model study. Palaeogeography, Palaeoclimatology, Palaeoecology 442, 96-109.

Dercourt, J., Gaetani, M., Vrielynk, B., Barrier, E., Biju-Duval, B., Brunet, M.F., Cadet, J.P., Crasquin, S., Sandulescu, M. (Eds.), 2000. Atlas Peri-Tethys, Palaeogeographical Maps (279 pp.).

Dewey, J.F., Helman, M.L., Turco, E., Hutton, D.H.W., Knott, S.D., 1989. Kinematics of the western Mediterranean. In: Coward, M.P., Dietrich, D., Park, R.G. (Eds.), Alpine Tectonics. Geological Society, London, Special Publication 45. London, pp. 265-283.

Di Geronimo, I., Fredj, G., 1987. Les fonds à Errina aspera et Pachylasma giganteum. Documents et Travaux de l'IGAL, 245-247.

Drury, A.J., Liebrand, D., Westerhold, T., Beddow, H.M., Hodell, D.A., Rohlfs, N., Wilkens, R.H., Lyle, M., Bell, D.B., Kroon, D., Pälike1, H., Lourens, L.J., 2021. Climate, cryosphere and carbon cycle controls on Southeast Atlantic orbital-scale carbonate deposition since the Oligocene (30–0 Ma). Climate of the Past, 17(5), 2091-2117. https://doi.org/10.5194/cp-17-2091-2021.

Ferrandini M., Ferrandini J., Loye-Pilot M.D., Butterlin J., Cravatte J., Janin M.C., 1998. Le Miocène du bassin de Saint-Florent (Corse): modalités de la transgression du Burdigalien supérieur et mise en évidence du Serravallien. [The Miocene of the Saint-Florent basin

(Corsica): the Upper Burdigalian trangression and evidence for the presence of the Serravallian]. Geobios 31, 125-137.

Ferrandini M., Galloni F., Babinot J.-F., Margerel J.-P., 2002. La plate-forme burdigalienne de Bonifacio (Corse du Sud): microfaune (foraminifères, ostracodes) et paléoenvironnements. - Rev. micropal. 45, 57-68.

Flügel, E., 2004. Microfacies of carbonate rocks. Springer, London, 976 pp.

Fredj, G., Giermann, G., 1982. Observations en soucoupe plongeante SP 300 des peuplements d'Errina aspera (L.) (Stylasterina) du de´troit de Messine. Téthys 10, 280-286.

Giacobbe, S., Laria, G., Spanò, N., 2007. Hard bottom assemblages in the Strait of Messina: distribution of *Errina aspera* L. (Hydrozoa: Stylasteridae). Rapport Commission International Mer Méditerranée 38, 485.

Gueguen, E., Doglioni, C., Fernandez, M., 1998. On the post-25 Ma geodynamic evolution of the western Mediterranean. Tectonophysics 298, 259-269.

Halfar, J., Godinez-Orta, L., Mutti, M., Valdez-Holguin, J.E., Borges, J.M., 2004. Nutrient and temperature controls on modern carbonate production: an example from the Gulf of California, Mexico. Geology 32, 213-216.

Halfar, J., Mutti, M., 2005. Global dominance of coralline red-algal facies: A response to Miocene oceanographic events. Geology 33, 481-484.

Halfar, J., Godinez-Orta, L., Mutti, M., Valdez-Holguin, J.E., Borges, J.M., 2006. Carbonates calibrated against oceanographic parameters along a latitudinal transect in the Gulf of California, Mexico. Sedimentology 53, 297-320.

Hallock, P., Schlager, W., 1986. Nutrient excess and the demise of coral reefs and carbonate platforms. Palaios 1, 389-398.

Hanes, D.M., Barnard, P.L., 2007. Morphological evolution in the San Francisco bight. Journal of coastal research 50, 469-473.

Harper, J.R., Henry, R.F. and Stewart, G.G., 1988. Maximum storm surges elevations in the Tuktoyaktuk region of the Canadian Beaufort Sea. Arctic, 41, 48-52.

Häussermann, V., Försterra, G., 2007. Extraordinary abundance of hydrocorals (Cnidaria, Hydrozoa, Stylasteridae) in shallow water of the Patagonian fjord region. Polar Biology, 30(4), 487-492.

Hemer, M.A., Harris, P.T., Coleman, R., Hunter, J., 2004. Sediment mobility due to currents and waves in the Torres Strait–Gulf of Papua region. Continental Shelf Research 24, 2297-2316.

Héquette, A., Hill, P.R., 1993. Storm-generated currents and offshore sediment transport on a sandy shoreface, Tibjak Beach, Canadian Beaufort Sea. Marine Geology, 113, 283-304.

Hine, A.C., Harris, M.W., Locker, S.D., Hallock, P., Peebles, M., Tedesco, L., Mullins, H.T., Snyder, S.W., Belknap, D.F., Gonzales, J.L., Neuman, A.C., 1994. Sedimentary infilling of an open seaway; Bawihka Channel, Nicaraguan Rise. Journal of Sedimentary Research 64, 2-25.

James, N.P., 1997. The cool-water carbonate depositional realm. In: James, N.P., Clarke, J.A.D. (Eds.), Cool-water carbonates. SEPM Special Publication 56, pp. 1-20.

James, N.P., Bone, Y., Kyser, T.K., 2005. Where has all the aragonite gone? Mineralogy of Holocene neritic cool-water carbonates, southern Australia. Journal of Sedimentary Research 75, 454-463.

James, N.P., Lukasik, J.J., 2010. Cool- and cold-water carbonates. In: James, N.P., Dalrymple, R.W. (Eds.), Facies Models 4. Geological Association of Canada, GEOtext 6, St John's, Newfoundland, pp. 371–399.

James, N.P., Seibel, M.J., Dalrymple, R.W., Besson, D., Parize, O., 2014. Warm-temperate, marine, carbonate sedimentation in an Early Miocene, tide-influenced, incised valley; Provence, south-east France. Sedimentology 61, 497-534.

Knoerich, A.C., Mutti, M., 2003. Controls of facies and sediment composition on the diagenetic pathway of shallow water Heterozoan carbonates: the Oligocene of the Maltese Islands. International Journal of Earth Sciences (Geologische Rundschau) 92, 494-510.

Knoerich, A.C., Mutti, M., 2006a. Missing aragonitic biota and the diagenetic evolution of heterozoan carbonates: a case study from the Oligo-Miocene of the central Mediterranean. Journal of Sedimentary Research 76, 871-888.

Knoerich, A.C., Mutti, M., 2006b. Epitaxial calcite cements in Earth history: a cooler-water phenomenon during aragonite-sea times? In: Pedley, H.M., Carannante, G. (Eds.), Cool-Water Carbonates: Depositional Systems and Palaeoenvironmental Controls. Geological Society, London, Special Publication 255, pp. 323-335.

Krautworst, U.M.R., Brachert, T.C., 2003. Sedimentary facies during early stages of flooding in an extensional basin: the Brèche Rouge de Carboneras (Late Miocene, Almería/SE Spain). International Journal of Earth Sciences (Geologische Rundschau) 92, 610-623.

Longhitano, S.G., 2011. The record of tidal cycles in mixed silici–bioclastic deposits: examples from small Plio–Pleistocene peripheral basins of the microtidal Central Mediterranean Sea. Sedimentology 58, 691-719.

Longhitano, S.G., 2013. A facies-based depositional model for ancient and modern, tectonically-confined tidal straits. Terra Nova 25, 446-452.

Longhitano, S.G., 2018a. Between Scylla and Charybdis (part 1): the sedimentary dynamics of the modern Messina Strait (central Mediterranean) as analogue to interpret the past. Earth-Science Reviews 185, 259-287.

Longhitano, S.G., 2018b. Between Scylla and Charybdis (part 2): The sedimentary dynamics of the ancient, Early Pleistocene Messina Strait (central Mediterranean) based on its modern analogue. Earth-Science Reviews 179, 248-286.

Longhitano, S.G., Chiarella, D., Di Stefano, A., Messina, C., Sabato, L., Tropeano, M., 2012a. Tidal signatures in Neogene to Quaternary mixed deposits of southern Italy straits and bays. Sedimentary Geology 279, 74-96.

Longhitano, S.G., Chiarella, D., Gugliotta, M., Ventra, D., 2021a. Coarse-grained deltas approaching shallow-water canyon heads: a case study from the Lower Pleistocene Messina Strait, Southern Italy. Sedimentology 68, 2523-2562.

Longhitano, S.G., Chiarella, D., Muto, F., 2014. Three-dimensional to two-dimensional cross-strata transition in the lower Pleistocene Catanzaro tidal strait transgressive succession (southern Italy). Sedimentology 61, 2136-2171.

Longhitano, S.G., Mellere, D., Steel, R.J., Ainsworth, R.B., 2012b. Tidal depositional systems in the rock record: a review and new insights. Sedimentary Geology 279, 2-22.

Longhitano, S.G., Rossi, V.M., Chiarella, D., Mellere, D., Tropeano, M., Dalrymple, R.W., Steel, R.J., Nappi, A., Olita, F., 2021b. Anatomy of a mixed bioclastic–siliciclastic regressive tidal sand ridge: Facies-based case study from the lower Pleistocene Siderno Strait, southern Italy. Sedimentology 68, 2293-2332.

Longhitano, S.G., Sabato, L., Tropeano, M., Gallicchio, S., 2010. A mixed bioclastic–siliciclastic flood-tidal delta in a micro-tidal setting: depositional architectures and hierarchical internal organization (Pliocene, Southern Apennine, Italy). Journal of Sedimentary Research 80, 36-53.

Longhitano, S.G., Telesca, D., Pistis, M., 2017. Tidal sedimentation preserved in volcaniclastic deposits filling a peripheral seaway embayment (early Miocene, Sardinian Graben). Marine and Petroleum Geology 87, 31-46.

Lund, M., Davies, P.J., Braga, J.C., 2000. Coralline algal nodules off Fraser Island, eastern Australia. Facies 42, 25-34.

Machel, H.G., 1985. Cathodoluminescence in calcite and dolomite and its chemical interpretation. Geoscience Canada 12, 139-147.

Maino, M., Decarlis, A., Felletti, F., Seno, S., 2013. Tectono-sedimentary evolution of the Tertiary Piedmont Basin (NW Italy) within the Oligo-Miocene central Mediterranean geodynamics. Tectonics 32, 593-619.

Malinverno, A., Ryan, W.B.F., 1986. Extension in the Tyrrhenian Sea and shortening in the Apennines as a result of arc migration driven by sinking of the lithosphere. Tectonics 5, 227-245.

Martín, J.M., Braga, J.C., Betzler, C., 2001. The Messinian Guadalhorce corridor: the last northern, Atlantic-Mediterranean gateway. Terra Nova 13, 418-424

Martín, J.M., Braga, J.C., Aguirre, J., Puga-Bernabéu, A., 2009. History and evolution of the North-Betic Strait (Prebetic Zone, Betic Cordillera): A narrow, early Tortonian, tidal-dominated, Atlantic-Mediterranean marine passage. Sedimentary Geology 216, 80-90.

Martín, J.M., Braga, J.C., Aguirre, J., Betzler, C., 2004. Contrasting models of temperate carbonate sedimentation in a small Mediterranean embayment: the Pliocene Carboneras Basin, SE Spain. Journal of the Geological Society London 161, 387-399.

Martín, J.M., Braga, J.C., Riding, R., 1997. Late Miocene *Halimeda* alga-microbial segment reefs in the marginal Mediterranean Sorbas Basin, Spain. Sedimentology 44, 441-456.

Martín, J.M., Puga-Bernabéu, Á., Aguirre J., Braga, J.C., 2014. Miocene Atlantic-Mediterranean seaways in the Betic Cordillera (Southern Spain). Revista de la Sociedad Geológica de España 27, 175-186.

Mastandrea, A., Muto, F., Neri, C., Papazzoni, C.A., Perri, E., Russo, F., 2002. Deep-Water Coral Banks: an Example from the "Calcare di Mendicino" (Upper Miocene, Northern Calabria, Italy). Facies 47, 27-42.

Mateu-Vicens, G., Hallock, P., Brandano, M., 2008. A depositional model and paleoecological reconstruction of the Lower Tortonian distally steepened ramp of Menorca (Balearic Islands, Spain). Palaios 23, 465-481.

Mateu-Vicens, G., Brandano, M., Gaglianone, G., Baldassarre, A., 2012. Seagrass-meadow sedimentary facies in a mixed siliciclastic-carbonate temperate system in the Tyrrhenian Sea (Pontinian Islands,Western Mediterranean). Journal of Sedimentary Research 82, 451–463.

Michel, J., Borgomano, J., Reijmer, J.J., 2018. Heterozoan carbonates: When, where and why? A synthesis on parameters controlling carbonate production and occurrences. Earth-Science Reviews 182, 50-67.

Mosbrugger, M., Uterscher, T., Dilcher, D.L., 2005. Cenozoic continental climatic evolution of Central Europe. Proc. Natl. Acad. Sci. U. S. A. 102, 14964–14969.

Mosca, P., Polino, R., Rogledi, S., Rossi, M., 2010. New data for the kinematic interpretation of the Alps-Apennines junction (Northwestern Italy). International Journal of Earth Sciences (Geologische Rundschau) 99, 833-849.

Mosna S., Seno S., Vanossi, M. 1990. Depositi postorogeni dell'Oligocene Inferiore interposti tra il Brianzonese e la "Pietra di Finale" (Alpi Liguri): conseguenze paleotettoniche e paleogeografiche. Atti Ticinesi Scienze della Terra 33, 11-21.

Mutti. E., Papani, L., Di Biase, D., Davoli, G., Mora, S., Segadelli, S., Tinterri, R., 1995. Il Bacino Terziario Epimesoalpino e le sue implicazioni sui rapporti tra Alpi ed Appennino. Memorie di Scienze Geologiche di Padova 47, 217-244.

Mutti, M., Hallock, P., 2003. Carbonate systems along nutrient and temperature gradients: some sedimentological and geochemical constraints. International Journal of Earth Sciences (Geologische Rundschau) 92, 465-475.

Nembrini, M., Berra, F., Della Porta, G., Fiorani, S., 2017. Facies characterization and depositional model of the Pietra di Finale Formation (Miocene, Liguria, N Italy). Journal of Mediterranean Earth Sciences 9, XIII Geosed Congress-Abstract, 185. https://doi.org/10.3304/JMES.2017.004.

O'Connell, L.G., James, N.P., Doubell, M., Middleton, J.F., Luick, J., Currie, D.R., Bone, Y., 2016. Oceanographic controls on shallow-water temperate carbonate sedimentation: Spencer Gulf, South Australia. Sedimentology 63, 105-135.

Oudet, J., Münch, P., Verati, C., Ferrandini, M., Melinte-Dobrinescu, M., Gattacceca, J., ... Ferrandini, J., 2010. Integrated chronostratigraphy of an intra-arc basin: 40Ar/39Ar datings, micropalaeontology and magnetostratigraphy of the early Miocene Castelsardo basin (northern Sardinia, Italy). Palaeogeography, Palaeoclimatology, Palaeoecology 295, 293-306.

Pedley, M., 1998. A review of sediment distribution and processes in Oligo-Miocene ramps of southern Italy and Malta (Mediterranean divide). In: Wright, V.P., Burchette, T.P. (Eds), Carbonate Ramps. Geological Society, London, Special Publication 149, pp. 163-179.

Pedley, M, Carannante, G., 2006. Cool-water carbonate ramps: a review. In: Pedley, H.M., Carannante, G. (Eds.), Cool-Water Carbonates: Depositional Systems and Palaeoenvironmental Controls. Geological Society, London, Special Publication 255, pp. 1-9.

Perrin, C., Bosellini, F.R., 2012. Paleobiogeography of scleractinian reef corals: changing patterns during the Oligocene–Miocene climatic transition in the Mediterranean. Earth-Science Reviews 111, 1-24.

Pomar, L., Ward, W.C., Green, D.G., 1996. Upper Miocene reef complex of the Llucmajor area, Mallorca, Spain. Models for Carbonate Stratigraphy from Miocene Reef Complexes of Mediterranean Regions, SEPM Concepts in Sedimentology and Paleontology 5, 191-225.

Pomar, L., Baceta, J.I., Hallock, P., Mateu-Vicens, G., Basso, D., 2017. Reef building and carbonate production modes in the west-central Tethys during the Cenozoic. Marine and Petroleum Geology 83, 261-304.

Pomar, L., Bassant, P., Brandano, M., Ruchonnet, C., Janson, X., 2012. Impact of carbonate producing biota on platform architecture: Insights from Miocene examples of Mediterranean region. Earth-Science Reviews 113, 186-211.

Pomar, L., Brandano, M., Westphal, H., 2004. Environmental factors influencing skeletal grain sediment associations: a critical review of Miocene examples from the western Mediterranean. Sedimentology 5, 627-651.

Pomar, L. Hallock, P., 2007. Changes in coral-reef structure through the Miocene in the Mediterranean province: adaptive versus environmental influence. Geology 35, 899-902.

Pomar, L., Kendall, C.G.S.C., 2008. Architecture of carbonate platforms: A response to hydrodynamics and evolving ecology. In: Lukasik, J., Simo, A. (Eds.), Controls on Carbonate Platform and Reef Development: SEPM Special Publication 89, pp. 187–216.

Pomar, L., Obrador, A., Westphal, H., 2002. Sub-wavebase cross-bedded grainstones on a distally steepened carbonate ramp, Upper Miocene, Menorca, Spain. Sedimentology 49, 139-169.

Popov, S.V., Rögl, F., Rozanov, A.Y., Steininger, F.F., Shcherba, I.G., Kovac, M., 2004. Lithological–paleogeographic maps of Paratethys, 10 maps late Eocene to Pliocene. Courier Forschungsinstitut Senckenberg 250, 1–46.

Pufahl, P.K., 2010. Bioelemental sediments. In: James, N.P., Dalrymple, R.W. (Eds.), Facies Models 4: Geological Association of Canada, GEOtext 6, St John's, Newfoundland, pp. 477–503.

Reading, H.G., Collins, J.D., 1996. Clastic coasts. In: Reading, H.G. (Ed.), Sedimentary Environments: Processes, Facies and Stratigraphy. Blackwell Science, Oxford, pp. 154-231.

Rehault, J.P., Boillot, G., Mauffret, A., 1984. The western Mediterranean basin geological evolution. Marine Geology 55, 447-477.

Reynaud, J.Y., Dalrymple, R.W., Vennin, E., Parize, O., Besson, D., Rubino, J.L., 2006. Topographic controls on production and deposition of tidal cool-water carbonates, Uzes Basin, SE France. Journal of Sedimentary Research 76, 117-130.

Reynaud, J.Y, James, N.P., 2012. The Miocene Sommières basin, SE France: Bioclastic carbonates in a tide-dominated depositional system. Sedimentary Geology 282, 360-373.

Reynaud, J.Y., Ferrandini, M., Ferrandini, J., Santiago, M., Thinon, I., André, J.P., Barthet, Y., Guennoc, P., Tessier, B., 2013. From non-tidal shelf to tide-dominated strait: The Miocene Bonifacio Basin, Southern Corsica. Sedimentology 60, 599-623.

Reynaud, J.Y., Tessier, B., Auffret, J.P., Berné, S., de Batist, M., Marsset, T., Walker, P., 2003. The offshore Quaternary sediment bodies of the English Channel and its Western Approaches. Journal of Quaternary Science: Published for the Quaternary Research Association, 18, 361-371.

Reynaud, J.Y., Vennin, E., Parize, O., Rubino, J.L. and Bourdillon, C., 2012. Incised valleys and tidal seaways: the example of the Miocene Uzès-Castillon basin, SE France. Bulletin de la Société Géologique de France 183, 471-486.

Roberts, J.M., Wheeler, A.J., Freiwald, A. 2006. Reefs of the deep: the biology and geology of cold-water coral ecosystems. Science 312, 543-547

Rooper, C.N., Zimmermann, M., Prescott, M.M., Hermann, A.J., 2014. Predictive models of coral and sponge distribution, abundance and diversity in bottom trawl surveys of the Aleutian Islands, Alaska. Marine Ecology Progress Series, 503, 157-176.

Rossi, V.M., Longhitano, S.G., Mellere, D., Dalrymple, R.W., Steel, R.J., Chiarella, D., Olariu, C., 2017. Interplay of tidal and fluvial processes in an early Pleistocene, delta-fed, strait margin (Calabria, Southern Italy). Marine and Petroleum Geology 87, 14-30.

Roveta, C., Bavestrello, G., Montefalcone, M., Pica, D., Puce, S., 2019. Asymmetrical distribution of *Distichopora violacea* (Cnidaria: Hydrozoa) in four Maldivian atolls. The European Zoological Journal, 86(1), 9-19.

Salvati, E., Angiolillo, M., Bo, M., Bavestrello, G., Giusti, M., Cardinali, A., Puce, S., Spaggiari, C., Greco, S., Canese, S., 2010. The population of *Errina aspera* (Hydrozoa: Stylasteridae)

of the Messina Strait (Mediterranean Sea). Journal of the Marine Biological Association of United Kingdom 90, 1331-1336.

Santoro, V.C., Amore, E., Cavallaro, L., Cozzo, G., Foti, E., 2002. Sand Waves in the Messina Strait, Italy. Journal of Coastal Research, Special Issue 36, 640-653.

Schlanger, S.O., Carroll, D., Hathaway, J.C., 1964. Petrology of the limestones of Guam. US Government Printing Office.

Slootman, A., De Boer, P.L., Cartigny, M.J., Samankassou, E., Moscariello, A., 2019. Evolution of a carbonate delta generated by gateway-funnelling of episodic currents. Sedimentology 66, 1302-1340.

Soria, J.M., Fernández, J., Viseras, C., 1999. Late Miocene stratigraphy and palaeogeographic evolution of the intramontane Guadix Basin (Central Betic Cordillera, Spain): implications for an Atlantic-Mediterranean connection. Palaeogeography, Palaeoclimatology, Palaeoecology 151, 255-266.

Speranza, F., Villa, I.M., Sagnotti, L., Florindo, F., Cosentino, D., Cipollari, P., Mattei, M., 2002. Age of the Corsica-Sardinia rotation and Liguro-Provençal Basin spreading: new paleomagnetic and Ar/Ar evidence. Tectonophysics 347, 231-251.

Stampfli, G.M., Marchant, R.H., 1997. Geodynamic evolution of the Tethyan margins of Western Alps. Deep Structure of the Swiss Alps-Results from NRP 20, 223-239.

Swart, P.K., 2015. The geochemistry of carbonate diagenesis: The past, present and future. Sedimentology 62, 1233-1304.

Tada, R., Siever, R., 1989. Pressure solution during diagenesis. Annual Review of Earth Planetary Sciences 17, 89-118.

Telesca, D., Longhitano, S.G., Pistis, M., Pascucci, V., Tropeano, M., Sabato, L., 2020. Sedimentology of a transgressive middle-upper Miocene succession filling a tectonically confined, current dominated seaway (the Logudoro Basin, northern Sardinia, Italy). Sedimentary Geology, 400, 105626.

Tomás, S., Zitzmann, M., Homann, M., Rumpf, M., Amour, F., Benisek, M., Marcano, G., Mutti, M., Betzler, C., 2010. From ramp to platform: building a 3D model of depositional geometries and facies architectures in transitional carbonates in the Miocene, northern Sardinia. Facies 56, 195-210.

Tomassetti, L., Brandano, M., 2013. Sea level changes recorded in mixed siliciclastic–carbonate shallow-water deposits: The Cala di Labra Formation (Burdigalian, Corsica). Sedimentary Geology 294, 58-67.

Tomassetti, L., Bosellini, F.R., Brandano, M., 2013. Growth and demise of a Burdigalian coral bioconstruction on a granite rocky substrate (Bonifacio Basin, southeastern Corsica). Facies 59, 703-716.

Tournadour, E., Fournier, F., Etienne, S., Collot, J., Mavrizet, P., Patriat, M., Sevin, B., Morgans, H.E.G., Martin-Garin, B., Braga, J. C. (2020). Seagrass-related carbonate ramp development at the front of a fan delta (Burdigalian, New Caledonia): Insights into mixed carbonate-siliciclastic environments. Marine and Petroleum Geology, 121, 104581.

Tucker, M.E., Wright, V.P., 1990. Carbonate Sedimentology. Blackwell Science Ltd, Oxford, U.K, 482 pp.

Vertino, A., 2003. Sclerattiniari Plio-Pleistocenici ed attuali del Mediterraneo (Sistematica, Biostratinomia e Paleoecologia). Unpublished PhD thesis. Italy: University of Messina 306.

Vertino, A., Stolarski, J., Bosellini, F.R., Taviani, M., 2014. Mediterranean corals through time: From Miocene to Present. In: Goffredo, S., Dubinsky, Z. (Eds), The Mediterranean Sea: Its History and Present Challenges. Springer Science+Business Media Dordrecht, Dordrecht, pp. 257-274.

Viana, A.R., Faugères, J.C., Stow, D.A.V., 1998. Bottom-current-controlled sand deposits - a review of modern shallow-to deep-water environments. Sedimentary Geology 115, 53-80.

Yalin, M.S., 1964. Geometrical properties of sand waves. Proc. Am. Soc. Civil Eng. 90, 105–119.

You, Y., Huber, M., Müller, R.D., Poulsen, C.J., Ribbe, J., 2009. Simulation of the middle Miocene climate optimum. Geophysical Research Letters 36, L04702, 1-5.

Yoshida, S., Steel, R.J., Dalrymple, R.W., 2007. Changes in depositional processes—an ingredient in a new generation of sequence-stratigraphic models. Journal of Sedimentary Research 77, 447-460.

Westphal, H., Halfar, J., Freiwald, A., 2010. Heterozoan carbonates in subtropical to tropical settings in the present and past. International Journal of Earth Sciences 99, 153-169.

Wilson, M.E.J., Vecsei, A., 2005. The apparent paradox of abundant foramol facies in low latitudes: their environmental significance and effect on platform development. Earth-Science Reviews 69, 133-168.

Zachos, J., Pagani, M., Sloan, L., Thomas, E., Billups, K., 2001. Trends, rhythms, and aberrations in global climate 65 Ma to present. Science 292, 686-693.

Zibrowius, H., Cairns, S.D., 1992. Revision of the northeast Atlantic and Mediterranean Stylasteridae (Cnidaria: Hydrozoa). Mémoires du Muséum d'Histoire Naturelle, Westerberg 153, 1-136.

Figure captions

Figure 1. A) Paleogeographic map of the Western Mediterranean at the early Langhian time redrafted after Dercourt et al. (2000) with integration from Dewey et al. (1989), Gueguen et al. (1998), Oudet et al. (2010), Reynaud and James (2012) and Reynaud et al. (2013). The red star indicates the approximate location of the Finale Ligure study area. B) Geological setting of the Ligurian Alps, Tertiary Piedmont Basin (TPB) and NW Apennines (redrafted after Maino et al., 2013), NW Italy (insert in the upper left corner). The Oligocene-Miocene sedimentary succession of the Finale Ligure study area (Finale Ligure Limestone and underlying terrigenous deposits labelled as Basal Complex by Boni et al., 1968) overlies the deformed Alpine tectonic units. The red rectangle identifies the Finale Ligure study area mapped in Figure 4.

Figure 2. Lithostratigraphic subdivision of the Oligocene-Miocene sedimentary succession of the Finale Ligure area deposited on the deformed Alpine tectonic units according to different authors. A) Stratigraphic diagram from North to South (close to B-B' line in Figure 4) redrafted after Boni et al. (1968, 1971) showing the stratigraphic relationships (wavy contacts are erosional surfaces) in the Verezzi area, SW of the Oligocene-Miocene Finale Ligure succession (for location refer to Figure 4). Boni et al. (1968) identified a "Basal Complex" of the Finale Ligure Limestone including: a) in the SW Verezzi outcrop, Oligocene polygenic conglomerate and sandstone and monogenic breccia with cobbles and boulders of the Triassic S. Pietro dei Monti Dolostone (Borgio Breccia); in the Mt. Cucco outcrop area, sandstone west of Mt. Cucco and S. Lorenzino Marl with uncertain stratigraphic position, probably Oligocene to lower Miocene. The Finale Ligure Limestone was subdivided in five members: a) marlstone and sandstone of the Torre di Bastia Mb., b) conglomerate of the Poggio Mb., and c) the three overlying units dominated by skeletal fragments are Verezzi Mb. (ca. 50 m thick), Rocce dell'Orera Mb. (ca. 70 m thick) and Mt. Cucco Mb. (ca. 200 m thick). B) Stratigraphic subdivision of the Finale Ligure Limestone labelled Pietra di Finale Fm., according to Brandano et al. (2015) comprising two units: a) the terrigenous unit, including the Poggio Mb. and the Torre di Bastia Mb. of Boni et al. (1968), and b) the calcareous

unit, including the Verezzi, Rocce dell'Orera and Mt. Cucco members of Boni et al. (1968). Depositional profile proposed by Brandano et al. (2015) for the Langhian-Serravallian calcareous unit of the Finale Ligure Limestone with spatial distribution of five lateral facies: F1 and F2 clast-supported conglomerate facies, F3 balanid facies, F4 *Halimeda* facies and F5 bivalve facies (redrafted after Brandano et al., 2015).

Figure 3. Outcrop photographs of the calcareous unit of the Finale Ligure Limestone. A) Panoramic view of the Rocca di Perti, Rocca Carpanea and Mt. Cucco ridges (cf. Fig. 4) from the West showing the southward tilting of the cross-bedded calcareous unit. B) Metre-scale cross-bedded facies at Rocca di Perti. The orange dashed lines identify the main, metre-scale bedding surfaces, dipping southward. C) Detail of cross-bedding with planar oblique lamination (green dashed lines) varying in dip angle and direction both southward (seaward) and northward (landward).

Figure 4. Geological map of the study area showing the traces of the geological cross-sections (Fig. 5) and the location of the measured stratigraphic logs (Fig. 6).

Figure 5. Geological cross-sections across the Finale Ligure Limestone (see Figure 4 for the geological cross-section traces and colour legend). The lighter transparent tones correspond to interpreted eroded deposits.

Figure 6. Selected stratigraphic logs showing vertical relationships among the lithofacies identified in the Oligocene-Miocene succession of Finale Ligure Limestone transgressive above the Alpine Units (see Figure 4 for location of the stratigraphic logs).

Figure 7. A) Outcrop photograph of L1 massive dolostone breccia, directly overlying the Alpine bedrock, composed of angular dolostone clasts of the Triassic S. Pietro dei Monti Dolostone Fm. (Verezzi area, Poggio; Fig. 4). B) L2 litharenite with quartz (Qz), metamorphic and carbonate rock fragments (Cf), glaucony grains (G) and calcite cement (Verezzi area, Bracciale; Fig. 4). C) Sand- to silt-grade litharenite (L3.1) with quartz (Qz), metamorphic and carbonate rock fragments and glaucony grains (black arrows), (Verezzi area, Torre di Bastia; Fig. 4). D) L3.2 laminated

packstone with planktonic foraminifera (black arrows), quartz (Qz), carbonate rock fragments, echinoid spines (Es) and glaucony (G), (Verezzi area, Torre di Bastia; Fig. 4). E) L3.2 packstone with planktonic and benthic foraminifera, carbonate clasts, glaucony (G), quartz grains and silicified brachiopod shell (white arrows) (cross-polarized light). F) Fine-grained L4 litharenite with Fe and Mn crusts (black arrow) (north of Mt. Cucco, S. Lorenzino; Fig. 4).

Figure 8. A) Angular unconformity between lithofacies L4 and the overlying skeletal grainstone/rudstone of lithofacies L14 (calcareous units of the Finale Ligure Limestone) cropping out between Feglino and S. Lorenzino (North of Mt. Cucco; Fig. 4). B) Erosional surface between lithofacies L4 (below) and lithofacies L5 (above) massive conglomerate, breccia and coarse litharenite, near S. Lorenzino. C) Cobbles of Alpine units in the conglomerate of lithofacies L5, Orco (northern margin of the Finale Ligure outcrop area; Fig. 4).

Figure 9. A) Outcrop photograph of the sharp, slightly erosional contact between L6 bioturbated litharenite with calcite-cemented burrows and L8 litharenites and conglomerate with skeletal fragments, passing gradually upward into L13 and L14 skeletal rudstone/grainstone (south of Rocca di Perti, S. Eusebio, Figs. 4, 6). B) L6 conglomerate with well-rounded carbonate clasts (Cf), cemented by blocky sparite at Rocca di Corno. C) L7 conglomerate/breccia resting upon the San Pietro dei Monti Dolostone of the Alpine bedrock (Verezzi area, Poggio; Fig. 4). D) L7 immature litharenite with quartz, carbonate rock fragments and intergranular micrite matrix (Verezzi area, Mt. Caprazoppa; Figs. 4, 6). E) L8 litharenite with quartz, metamorphic rock fragments, sparse bivalves, brachiopods and barnacles (Mt. Tolla, southern margin of the Finale Ligure Limestone outcrop area; Fig. 4). F) L9 immature fine-grained litharenite with quartz, metamorphic and carbonate rock fragments, textularid (white arrow) and planktonic (black arrow) foraminifera filled by glaucony (Verezzi area, Torre di Bastia; Fig. 4).

Figure 10. A) Outcrop photograph of lithofacies L10 skeletal packstone/rudstone rich in pectinid bivalves (black arrows) (Verezzi area, Mt. Caprazoppa; Fig. 4). B) Lithofacies L10 tabular bidirectional crossbedding). C) Lithofacies L11 skeletal packstone with bivalves, barnacles,

bryozoans, planktonic (black arrows) and benthic foraminifera, red algae fragments (white arrows) and quartz grains. On the left, an irregular red colour Fe oxide-stained laminar calcrete crust embedding quartz grains in the central upper part (Verezzi area, Campi d'Orsi; Figs. 4, 6). D) Lithofacies L11 packstone with planktonic foraminifera (*Orbulina universa;* Ou), at Campi d'Orsi. E) Skeletal packstone with bryozoans (Bz), crinoids (Cr), echinoid spines (Es), benthic foraminifera, detrital grains, phosphate pellets and micrite matrix (lithofacies L12 at Verezzi, Campi d'Orsi; Fig. 4). F) Skeletal packstone with benthic foraminifera *Amphistegina* (Am), echinoderms, bryozoans, quartz and lithic fragments (lithofacies L12 north of Mt. Cucco, S. Lorenzino; Fig. 4).

Figure 11. A) Lithofacies L12 skeletal packstone with bivalves, brachiopods, crinoids, bryozoans, rare red algae fragments with borings (Ra), benthic foraminifera and rare scleractinian and stylasterid coral fragments. B) Lithofacies L13 grainstone with interparticle, intraparticle and vuggy porosity (blue epoxy) dominated by fragments of barnacles (B) with rare stylasterid corals, Rocca di Corno. C) L13 grainstone to packstone dominated by fragments of barnacles (B) with rare planktonic foraminifera (Pf) and red algae (Ra) (Verezzi area, Campo d'Orsi). D) Compound cross-bedding with planar lamination dipping in multiple directions (L14). E) Cross-bedded lithofacies L14 with aligned pebbles at the base (L8, white arrow), bidirectional lamination and trough cross lamination. F) Flaser to wavy bedding in L14 overlying a sharp erosional surface. G) Cross-bedding with planar oblique lamination dipping southward (seaward) and northward (landward). H) Trough cross-lamination showing forseset dipping in multiple directions in L14.

Figure 12. A) Lithofacies F14 grainstone with stylasterid corals (white arrow pointing to tubular cavities in oblique section) and scleractinian coral (black arrow, probable Dendrophylliidae) associated with oysters (Oy). B) L14 grainstone with stylasterid corals (white arrow pointing to possible gastrostyle), scleractinian coral (possible Caryophylliidae, black arrow) and oyster fragments (Oy) (Rocca di Corno; Fig. 4). C) L14 rudstone to boundstone with barnacles (B), echinoid spines (Es), scleractinian corals (black arrow points to possible Dendrophylliidae) and

stylasterid corals (white arrows). D) Transversal sections of stylasterid corals with white arrows pointing to possible cyclosystems. E) Transversal sections of stylasterid corals in grainstone with barnacle fragments. F) Grainstone/packstone to rudstone with stylasterid corals, detrital grains and sparse micrite with rare planktonic foraminifera (Pf) and ostracods (L14 at Roman Quarries; Fig. 4). The white arrow points to a possible gastrostyle in a longitudinal section of stylasterid coral. G) Oblique section of a stylasterid coral showing the meshwork of tiny coenosteal canals. H) Stylasterid corals in oblique and transversal sections associated with one *Amphistegina* foraminifer (Am).

Figure 13. A) Lithofacies L14 skeletal grainstone to rudstone with stylasterid corals (white arrows), barnacles (B), detrital quartz grains and intraparticle and interparticle porosity. Skeletal grains are lined by isopachous fibrous cement followed by scalenohedral overgrowth (sc). B) Bladed scalenohedral calcite cement (sc) between an oyster fragment (Oy), scleractinian (black arrow) and stylasterid (white arrows) corals, lined by Fe oxides in the open interparticle pore space indicative of meteoric diagenesis (lithofacies L14 at Rocca di Corno). C) Crossed-polarizers image of scalenohedral and blocky calcite cement in intra- and interparticle porosity between oyster fragments (Oy) and stylasterid corals (white arrows) (lithofacies L14 at Rocca di Corno). D) Isopachous fibrous marine cement (white arrows) enveloping bryozoan fragments (Bz), documenting reworking of skeletal grains after the precipitation of a first phase of marine cement and re-deposition in a micrite-rich low-energy environment (lithofacies L12 at Bric Spaventaggi). E) Biomoulds of barnacles (B) and echinoid spines filled by phreatic meteoric blocky sparite. Dissolution of skeletal fragments was followed by the precipitation of blocky sparite within the mouldic porosity (lithofacies L12 at S. Lorenzino). F) Cathodoluminescence photomicrograph showing the replacement of barnacle fragment (L12) by luminescent and blotchy luminescent sparite during meteoric and shallow burial diagenesis.

Figure 14. $\delta^{13}C$ vs. $\delta^{18}O$ (V-PDB) values of the investigated lithofacies. Most of the samples, with exception of lithofacies L3.1 and L9, show highly negative $\delta^{13}C$ and $\delta^{18}O$ values with

respect to expected marine values (red dotted ellipse), suggesting alteration during meteoric diagenesis as confirmed by the ^{13}C depleted isotopic signature of lithofacies F11 laminar calcrete crusts. Few lithofacies (L3.1, L9) show isotope values close to marine pristine values (blue dotted ellipse). Other samples (L1 breccia clasts, L3.2, L14) seem to record only a burial diagenetic signature with decreasing $\delta^{18}O$ and unaltered $\delta^{13}C$ with respect to expected marine values.

Figure 15. 3D reconstruction of the Finale Ligure Basin, obtained by the interpolation of the geological boundaries from the geological map in Figure 4 and a network of geological cross sections A) View from the south of the 3D model with the inferred original extension of the Finale Ligure Limestone (light yellow colour) and the network of geological cross sections (traces in red) used to produce the model. B) View of the contour lines of the base of the Finale Ligure embayment: note the narrow strait that connected the embayment with the open sea to the south, reconstructed according to the constraints form the outcrops of the Alpine unit bedrock. C) Lateral overview of the Miocene Finale Ligure basin: the black line (obtained by the intersection between the basal surface of the Finale Ligure Limestone succession and its topmost surface) marks the possible extension of the Langhian-Serravallian basin, connected to the open sea by a narrow strait; in yellow the intersection between the basal surface and the DEM (i.e., base of the Finale Ligure Limestone succession). The images, obtained with Move™, have a vertical exaggeration of 1.5.

Table 1. Description of terrigenous lithofacies type L1-L4 below the angular unconformity (CL = cathodoluminescence).Table 2. Description of terrigenous lithofacies L5-L7 and mixed skeletal carbonate-siliciclastic lithofacies L8-L14 (Finale Ligure Limestone) above the angular unconformity (CL = cathodoluminescence).

Table 1S. Supporting Online Information. Stable isotope O and C measurements of the investigated Oligocene-Miocene lithofacies.

Declaration of interests

☒The authors declare that they have no known competing financial interests or personal relationships that could have appeared to influence the work reported in this paper.

☐The authors declare the following financial interests/personal relationships which may be considered as potential competing interests:

Table 1 Description of terrigenous lithofacies type L1-L4 below the angular unconformity (CL = cathodoluminescence).

Facies type	Texture and components	Sedimentary structures	Thickness and spatial distribution	Diagenetic features	Depositional environment, previous authors' attribution and age
L1 Massive dolostone breccia	Clast-supported, poorly sorted, monomictitc breccia with angular pebbles and cobbles of dolostone with argillaceous and detrital carbonate matrix.	Massive discontinuous lenses.	90-100 m thick. Only in the SW Verezzi outcrops near Poggio and Piazza overlying Alpine bedrock.	Fe oxide crusts; mouldic and vuggy porosity due to meteoric dissolution of dolomite clasts.	Erosion of the Triassic S. Pietro dei Monti Dolostone after Alpine tectonic uplift forming karstic breccias. *Borgio Breccia of undetermined age, probably Oligocene according to Boni et al. (1968).*
L2 Glaucony-bearing litharenite and conglomerate	Beds of clast-supported, poorly-sorted litharenite (70% of L2 in volume) and conglomerate (30% of L2 in volume) with sub-rounded, granules and coarse sand-size grains with calcite cement. Mono- and polycrystalline quartz, plagioclase, carbonate clasts (mudstone, peloidal grainstone, dolostone), metamorphic rocks, glaucony grains. Sparse planktonic foraminifera filled by glaucony.	Planar beds (50-60 cm thick).	10-15 m thick. Only in the SW Verezzi outcrops near Bracciale, overlying Alpine bedrock and underlying L3.	Interparticle space with non-luminescent equant calcite cement and sparse clay matrix. Some carbonate clasts bright luminescent under CL. Elongated and concavo-convex grain contacts indicative of mechanical compaction preceding cementation.	Open marine shelf setting reworking terrigenous input from the Alpine bedrock; probable transgressive lag during marine flooding of the incised Alpine bedrock. *Polygenic conglomerate and sandstone (Bracciale) of Oligocene age according to Boni et al. (1968).*
L3 alternating L3.1 and L3.2 **L3.1 Litharenite and siltstone**	Grain- to matrix-supported litharenite with angular clasts, medium sand to silt grain size, with lenses of coarse sandstone, 3-4 cm thick, alternating with L3.2. Components: quartz, micas, glaucony pellets, carbonate clasts, detrital rhombohedral dolomite crystals, mudstone rip-up clasts. Rare benthic and planktonic foraminifera (*Globigerinoides* and *Praeorbulina*).	Planar beds (2-20 cm thick), fining upward, erosional bases; horizontal lamination, burrows due to bioturbation.	Cumulative L3.1 and L3.2 about 30 m thick. Only in the SW Verezzi outcrops near Torre di Bastia Hill.	Interparticle space with micrite to marly matrix with patchy luminescence. Silicification with chalcedony within inter- and intraparticle space of skeletal fragments (foraminifera). Evidence of compaction (concavo-convex and sutured grain contacts).	Open marine shelf environment with turbidite and hemipelagic fall-out sedimentation. Detrital grains from the Alpine bedrock. Planktonic foraminifera indicative of early Miocene age. *Torre di Bastia Mb. of the Finale Ligure Limestone of early Miocene to possibly basal Langhian age according to Boni et al. (1968).*
L3.2 Packstone-wackestone with planktonic foraminifera and fine grained litharenite	Packstone-wackestone with planktonic and benthic foraminifera (filled by glaucony), crinoids, echinoid spines, brachiopods and bivalves alternating with L3.1. Silt and fine sand grade litharenite with quartz, muscovite, carbonate clasts, glaucony grains. Benthic foraminifera: *Cibicides, Gyroidina, Pulleatina, Nodosaria, Lenticulina.* Planktonic foraminifera:	Planar beds (1-15 cm thick); bioturbation.	Cumulative L3.1 and L3.2 about 30 m thick. Only in the SW Verezzi outcrops near Torre di Bastia Hill.	Marly and micrite matrix recrystallized in microsparite with patchy luminescence. Silicification with chalcedony within pores and on calcite shells (foraminifera and	Open marine shelf environment with turbidite and hemipelagic fall-out sedimentation. Glaucony suggests low sedimentation rates. Planktonic and benthic foraminifera indicative of early Miocene age. *Torre di Bastia Mb. of*

	Globoquadrina praedehiscens, Globoquadrina dehiscens, Globigerinoides trilobus, Globoquadrina s.p., *Globigerinoides* s.p., *Paragloborotalia nana, P. semivera, P. acrostoma, Globigerina venezuelana*, *Praeorbulina.*			brachiopods).	*the Finale Ligure Limestone of early Miocene to possibly basal Langhian age according to Boni et al. (1968).*
L4 Litharenite alternating with green claystone	Grain-supported, well-sorted litharenite with clay matrix and micrite/microsparite, from angular to rounded detrital grains, coarse to fine sand grade. Detrital grains of quartz, metamorphic rocks, plagioclase and micas. Litharenite alternating with claystone beds. Erosional surface and angular unconformity at the top.	Planar beds (sandstone 1-2 m thick; claystone 5-60 cm thick). Lamination; bioturbation.	1-20 m thick. Only in the N, in the Mt. Cucco outcrops, along the road from Orco to Feglino and near San Lorenzino	Interparticle space with clay or marly matrix or microsparite. All non-luminescent components under CL. Fe oxides and Mn crusts in hardgrounds.	Undetermined shelf environment with siliciclastic input from the Alpine bedrock. *Sandstone and Marls West of Mt. Cucco (Oligocene to probably early Miocene) and S. Lorenzino Marls (Oligocene) according to Boni et al. (1968).*

Table 2. Description of terrigenous lithofacies L5-L7 and mixed skeletal carbonate-siliciclastic lithofacies L8-L14 (Finale Ligure Limestone) above the angular unconformity (CL = cathodoluminescence).

Facies type	Texture and components	Sedimentary structures	Thickness and spatial distribution	Diagenetic features	Depositional environment, previous authors' attribution and age
L5 Massive conglomerate, breccia and coarse litharenite	L5a) Coarse breccia, grain-supported, poorly sorted with angular to sub-angular clasts, cobbles and boulders (up to 2-3 m). Clasts of Permian-Carboniferous metamorphic rocks. L5b) Conglomerate and coarse litharenite, grain-supported, moderately sorted; clasts of sub-rounded to rounded, granules size quartz, carbonate (mudstone and dolostone) and metamorphic rocks.	Massive, lacking sedimentary structures.	3.5 m thick. L5a overlies L4 through erosional unconformity at S. Lorenzino. L5b crops out N of Rocca Carpanea.	Interparticle space with blocky cement non-luminescent to bright luminescent, after mechanical compaction, sparse microsparite and marly matrix. Blotchy luminescent scalenohedral cement before blocky sparite. Clasts are dissolved (mouldic porosity), oxidized and fractured with cement filling.	Coarse detrital deposits probably formed at the base of erosional cliffs at the N margin of the Finale Ligure basin. *Included in Polygenic conglomerate and sandstone (Ansaldo) of Oligocene age by Boni et al. (1968).*
L6 Burrowed litharenite and conglomerate	L6a) Grain-supported, moderate- to well-sorted burrowed litharenite (immature to well-cemented); L6b) conglomerate, rounded medium-coarse sand and granules of quartz (mono and polycrystalline), metamorphic rocks, plagioclase, mica, and carbonate rock fragments (dolostone, mudstone, peloidal packstone-grainstone). Rare echinoids, planktonic foraminifera and glaucony pellets.	Beds 0.4-2 m thick. L6a: bioturbation, cemented cm- to dm-size burrows. L6b: erosional base, fining upward.	30-40 m thick. L6 crops out in the W at S. Eusebio and at Rocca di Corno; L6 overlain by L8 through sharp erosional contact.	Differential calcite cementation in burrows. Main cement equant mosaic of non-luminescent sparite with blocky or drusy fabric. Dissolution vugs and moulds filled by blocky sparite cement.	Burrowed sandstone indicative of low-energy shelf overlying transgressive ravinement lag conglomerate. *Included in Polygenic conglomerate and sandstone (Perti) of Oligocene age by Boni et al. (1968).*
L7 Conglomerate and litharenite	Grain- to matrix-supported, poorly-sorted conglomerate, breccia and litharenite with intergranular matrix and sparse calcite cement, rounded to subangular clasts of coarse sand, granule and pebble size of quartz, carbonate rocks (peloidal grainstone-packstone, mudstone, dolostone) and metamorphic rock fragments, glaucony pellets. Rare skeletal grains: benthic foraminifera (textularids) and bryozoans.	Beds 2-5 m thick, inverse grading, planar lamination, tabular cross-bedding	50 m thick. L7 crops out in the SW Verezzi outcrops, near Poggio; L7 overlain by L8 through erosional contact.	Matrix (clay to micrite and bright luminescent microsparite) and blocky cement; scalenohedral calcite either bright luminescent or non-luminescent. Dissolution: mouldic and vuggy porosity with drusy sparite filling and clay coatings around grains. Concavo-convex grain contacts.	Basal transgressive ravinement lag reworking the Alpine bedrock. *Poggio Mb. of the Finale Ligure Limestone, early Miocene in age according to Boni et al. (1968).*
L8 Bedded litharenite and conglomerate with skeletal fragments	Grain-supported, immature with matrix and sparse cement, poorly-sorted conglomerate to litharenite, with rounded to sub-angular clasts of pebble, granule and coarse-medium sand of quartz, mica, carbonate and metamorphic rock fragments. Sparse bioclasts of brachiopods, bryozoans, barnacles, bivalves with microborings, echinoids and textularid foraminifera.	Beds 0.1-2 m thick. Planar cross-lamination.	0.1-30 m thick. L8 in discontinuous lenses, overlying Alpine bedrock or facies L6 or L7, and alternating with L12-14 in dm-thick beds.	Micrite matrix recrystallized in microsparite, sparse blocky mosaics of equant cement and scalenohedral cement with Fe oxide staining. Micritization and recrystallization of bioclasts. Mouldic porosity after clast dissolution. Evidences of compaction and pressure solution (concavo-convex and sutured contacts, stylolites).	Ravinement lag with onset of increased skeletal production or pulses of detrital input within confined current-dominated embayment at base of subaqueous dunes. *Rocce dell'Orera and Monte Cucco Mb. of the Finale Ligure Limestone of Langhian-Serravallian age in Boni et al. (1968); facies F1-F2 in Brandano et al. (2015).*
L9 Fine litharenite and siltstone with skeletal fragments	Matrix-supported, immature, fine litharenite and siltstone with marly matrix and clasts of angular quartz, metamorphic rock fragments, carbonate and sandstone intraclasts. Sparse planktonic and benthic (textularids) foraminifera infilled by glaucony, bryozoans and rare red algae fragments; phosphate and glaucony pellets.	Beds 1-2 m thick, planar lamination. Hardgrounds with Fe-Mn crusts; inverse grading, erosional surfaces.	L9 (2-4 m thick) crops out in the SW Verezzi outcrops in metre scale beds near Mt. Caprazoppa.	Fe oxides as grain coatings and in matrix (micrite and neomorphic microsparite due to recrystallization). Mouldic porosity after detrital grains.	Temporary low-energy conditions due to stasis of subaqueous dune migration; hardgrounds and glaucony due to low sedimentation rates; erosional surfaces due to resumed current traction. *Rocce dell'Orera Mb. of the Finale Ligure Limestone of Langhian-Serravallian age in Boni*

					et al. (1968).
L10 Skeletal packstone/ grainstone to rudstone with pectinids	Packstone/grainstone to rudstone with variable sparite cement and micrite matrix and skeletal fragments: pectinids and other bivalves, barnacles, bryozoans (infilled with glaucony), brachiopods, echinoid spines, crinoids, textularids, nodosarids and planktonic foraminifera. Sand-sized quartz, carbonate and metamorphic rock fragments and glaucony pellets.	Beds 0.1-0.3 m thick. Horizontal, tabular compound cross-bedding; bidirectional cross-lamination.	5-15 m thick. L10-L13 70-80 m thick in SW Verezzi outcrop near Mt. Caprazoppa.	Equant blocky sparite and microsparite as cement. Micritized and recrystallized skeletal grains. Interparticle, intraparticle and mouldic porosity after detrital grain erosion.	Subaqueous dunes in current-dominated embayment; the location in the SW and the presence of planktonic foraminifera, pectinids and glaucony suggest distal setting, more open marine with respect to L12-L14. *Verezzi Mb. of the Finale Ligure Limestone of Langhian-Serravallian age in Boni et al. (1968); facies F5 in Brandano et al. (2015).*
L11 Skeletal packstone with planktonic foraminifera	Packstone with bivalves, bryozoans, barnacles, echinoid spines, brachiopods, common planktonic foraminifera (*Globigerinoides, Praeorbulina, Orbulina universa*), rare benthic foraminifera (nodosarids, miliolids, textularids, *Elphidium, Amphistegina*), rare red algae (*Lithophyllum*), ostracods, gastropods. Bioclasts appear abraded; sand-sized quartz and metamorphic rock fragments.	Beds 1 m thick. Locally planar lamination.	2 m thick. L10-L13 70-80 m thick in SW Verezzi outcrop near Mt. Caprazoppa.	Micritization and Fe oxide staining. Dissolution (moulds and vugs) and pressure solution (sutured grain contacts, stylolite). Micrite and skeletal components patchy luminescent. Fe oxide rich paleosols (laminar calcrete crusts bright luminescent with alveolar fabric) with terrigenous lenses at the top.	Subaqueous dunes with reworked shallow-water bioclasts mixed with middle Miocene planktonic foraminifera. Calcrete indicative of subaerial exposure due to tectonic uplift. *Rocce dell'Orera Mb. of the Finale Ligure Limestone Langhian-Serravallian age in Boni et al. (1968).*
L12 Skeletal packstone/ rudstone	Packstone to rudstone, rare grainstone. Skeletal fragments: echinoids, crinoids, bryozoans, oysters, other bivalves, brachiopods, barnacles, rare red algae (*Lithophyllum*), benthic foraminifera (textularids, miliolids, *Amphistegina, Elphidium*), scleractinian and stylasterid corals, associated with sand-size quartz, metamorphic and carbonate rock fragments, rare glaucony and phosphate pellets. Echinoderms, bivalves and red algae with microborings. Alternating quartz-rich and bioclasts-rich beds (1-2 cm thick).	Beds 0.1-0.3 m to 1 m thick, horizontal to tabular compound cross-bedding, bidirectional and trough cross-lamination.	5-15 m thick in Rocca di Perti and Mt. Cucco; in SW Verezzi area L12 nearly 10 m thick; L8-13 nearly 100 m thick.	Micritized and microbored bioclasts, patchy luminescent. Relict isopachous fibrous cement around bioclasts embedded in micrite; rare scalenohedral and blocky calcite cement. Concavo-convex grain contacts; stylolites. Mouldic, vuggy, inter- and intra-particle porosity. Aragonitic skeletal fragments dissolved or replaced by blocky sparite.	Seaward migrating subaqueous dunes in confined embayment with reworked skeletal fragments partially lined by early marine cement. *Rocce dell'Orera and Monte Cucco Mb. of the Finale Ligure Limestone Langhian-Serravallian age in Boni et al. (1968); facies F3 in Brandano et al. (2015).*
L13 Barnacle grainstone/ rudstone	Grainstone to rudstone dominated by barnacles, echinoid spines, bryozoans, bivalves, crinoids, rare scleractinian and stylasterid corals, sparse sand-size quartz, metamorphic and carbonate rock fragments. In the Verezzi area grainstone to packstone with rare benthic and planktonic foraminifera (*Praeorbulina, Globigerinoides*) and red algae fragments.	Beds 0.05-1 m thick to 5-10 m bed sets, tabular compound cross-bedding, oblique, herringbone and trough cross lamination, flaser, wavy bedding.	L13-L14 (+L8) 150 m thick in Rocca di Perti and Mt. Cucco. In SW Verezzi L13 10 m thick; L8-13 nearly 100 m thick.	Micritized and microbored bioclasts, patchy luminescent. Isopachous fibrous cement around bioclasts, scalenohedral and blocky calcite cement. Fe oxides in Verezzi area. Mouldic and vuggy porosity associated with inter- and intra-particle porosity.	Seaward migrating subaqueous dunes of skeletal carbonate sand in confined embayment. *Monte Cucco Mb. of the Finale Ligure Limestone Langhian-Serravallian age in Boni et al. (1968); facies F3 in Brandano et al. (2015).*
L14 Skeletal grainstone to rudstone with corals	Grainstone to rudstone, locally boundstone, and rare packstone. Skeletal fragments: common scleractinian corals (Dendrophylliidae, Caryophylliidae), stylasterid corals (encrusting scleractinian corals, bryozoans), barnacles, bivalves, oysters, gastropods, bryozoans, echinoid spines, crinoids, brachiopods, ostracods, rare benthic foraminifera (*Amphistegina*, *Lenticulina*) and red algae, very rare planktonic foraminifera. Sparse sand-size quartz, metamorphic and carbonate	Beds 0.05-1 m thick to 5-10 m bed sets, tabular compound cross-bedding, oblique, herringbone and trough cross lamination, flaser, wavy bedding, erosional	L13-L14 (+L8) 150 m thick in Rocca di Perti and Mt. Cucco.	Micritized and microbored bioclasts, patchy luminescent. Isopachous fibrous and/or scalenohedral cements followed by blocky sparite locally with drusy fabric. Fe oxides line scalenohedral cement. Mouldic vuggy, inter- and intraparticle porosity. Aragonitic skeletal fragments replaced by blocky sparite. Micrite geopetal infill within	Seaward migrating subaqueous dunes of skeletal carbonate sand in confined embayment. *Monte Cucco Mb. of Finale Ligure Limestone of Langhian-Serravallian age in Boni et al. (1968); facies F4 in Brandano et al. (2015).*

	rock fragments, rare glaucony pellets.	surfaces.	corals. Mechanical compaction and pressure solution with stylolites before calcite cementation.

Highlights

- Flooding of eroded Alpine bedrock during the early Miocene produced a confined embayment
- Finale Ligure Limestone as example of mixed heterozoan carbonates and siliciclastics
- Confined embayments witness the amplification of tidal and storm currents
- Subaqueous dune of skeletal sands with abundant barnacle and stylasterid corals
- Previous *Halimeda* algae determination are revised as stylasterid corals

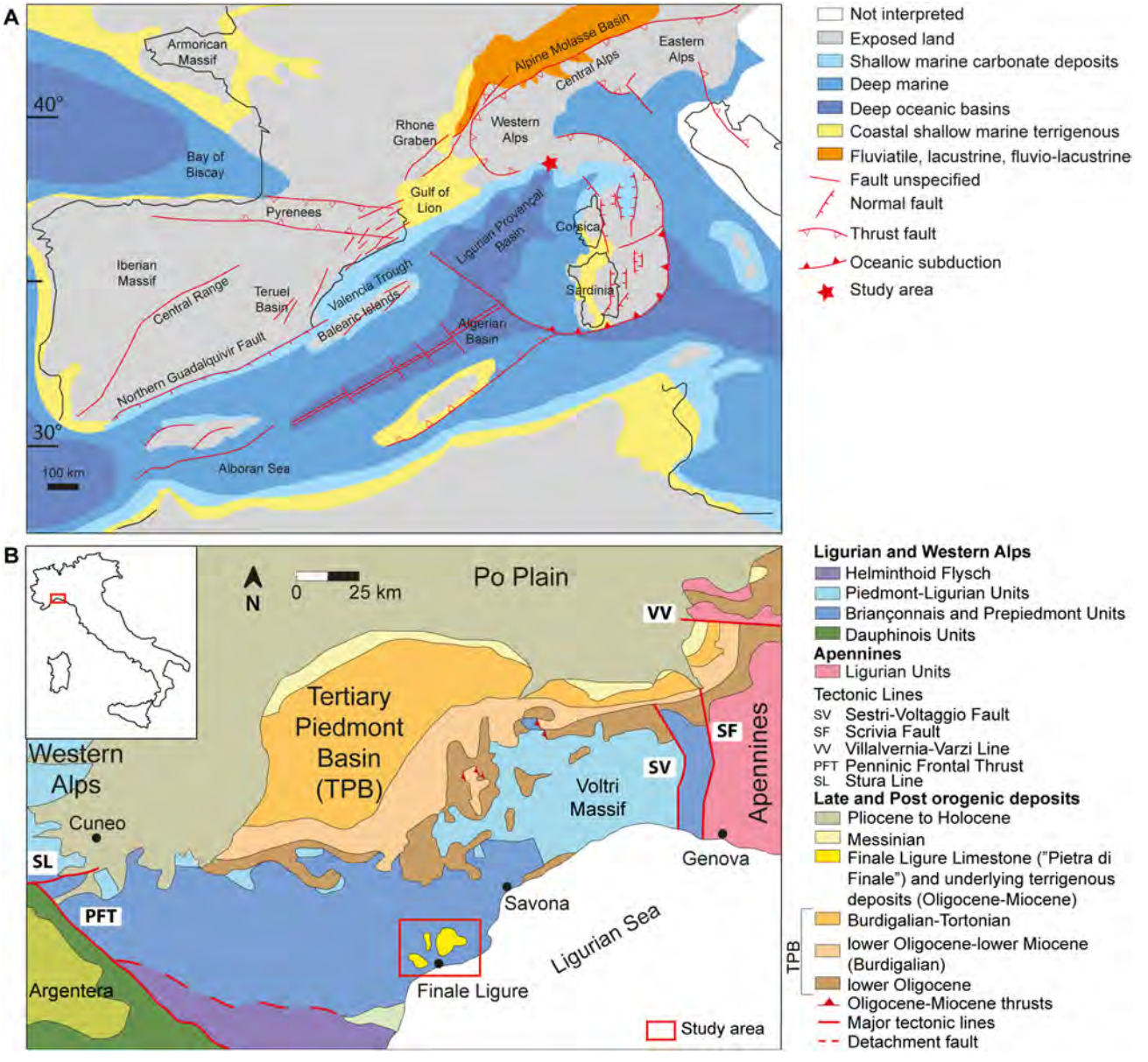
A
Armorican Massif
Alpine Molasse Basin
Central Alps
Eastern Alps
40°
Rhone Graben
Western Alps
Bay of Biscay
Gulf of Lion
Pyrenees
Ligurian Provençal Basin
Corsica
Iberian Massif
Central Range
Teruel Basin
Valencia Trough
Balearic Islands
Sardinia
Algerian Basin
Northern Guadalquivir Fault
30°
100 km
Alboran Sea
Not interpreted
Exposed land
Shallow marine carbonate deposits
Deep marine
Deep oceanic basins
Coastal shallow marine terrigenous
Fluviatile, lacustrine, fluvio-lacustrine
Fault unspecified
Normal fault
Thrust fault
Oceanic subduction
Study area
B
N
0
25 km
Po Plain
VV
Tertiary Piedmont Basin (TPB)
SF
SV
Voltri Massif
Apennines
Western Alps
Cuneo
SL
PFT
Genova
Savona
Ligurian Sea
Argentera
Finale Ligure
Study area
Ligurian and Western Alps
Helminthoid Flysch
Piedmont-Ligurian Units
Briançonnais and Prepiedmont Units
Dauphinois Units
Apennines
Ligurian Units
Tectonic Lines
SV Sestri-Voltaggio Fault
SF Scrivia Fault
VV Villalvernia-Varzi Line
PFT Penninic Frontal Thrust
SL Stura Line
Late and Post orogenic deposits
Pliocene to Holocene
Messinian
Finale Ligure Limestone ("Pietra di Finale") and underlying terrigenous deposits (Oligocene-Miocene)
TPB
Burdigalian-Tortonian
lower Oligocene-lower Miocene (Burdigalian)
lower Oligocene
Oligocene-Miocene thrusts
Major tectonic lines
Detachment fault

Figure 1

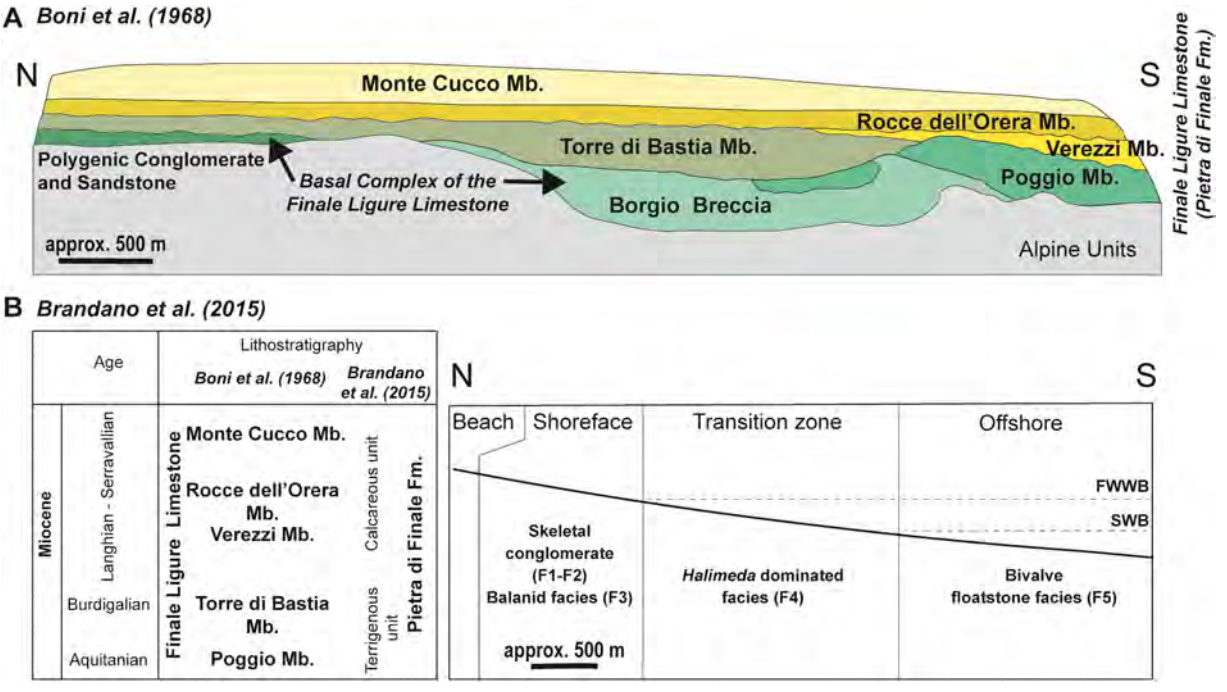
A Boni et al. (1968)
N
S
Monte Cucco Mb.
Rocce dell'Orera Mb.
Torre di Bastia Mb.
Verezzi Mb.
Poggio Mb.
Polygenic Conglomerate and Sandstone
Basal Complex of the Finale Ligure Limestone
Borgio Breccia
approx. 500 m
Alpine Units
Finale Ligure Limestone (Pietra di Finale Fm.)
B Brandano et al. (2015)
Age
Lithostratigraphy
Boni et al. (1968)
Brandano et al. (2015)
Miocene
Langhian - Serravallian
Burdigalian
Aquitanian
Finale Ligure Limestone
Monte Cucco Mb.
Rocce dell'Orera Mb.
Verezzi Mb.
Torre di Bastia Mb.
Poggio Mb.
Calcareous unit
Terrigenous unit
Pietra di Finale Fm.
N
S
Beach
Shoreface
Transition zone
Offshore
FWWB
SWB
Skeletal conglomerate (F1-F2)
Balanid facies (F3)
Halimeda dominated facies (F4)
Bivalve floatstone facies (F5)
approx. 500 m

Figure 2


A
N
S
Alpine Units
Rocca di Perti
B
Mt. Cucco
S. Eusebio
100 m
B
N
S
C
10 m
C
3 m

Figure 3

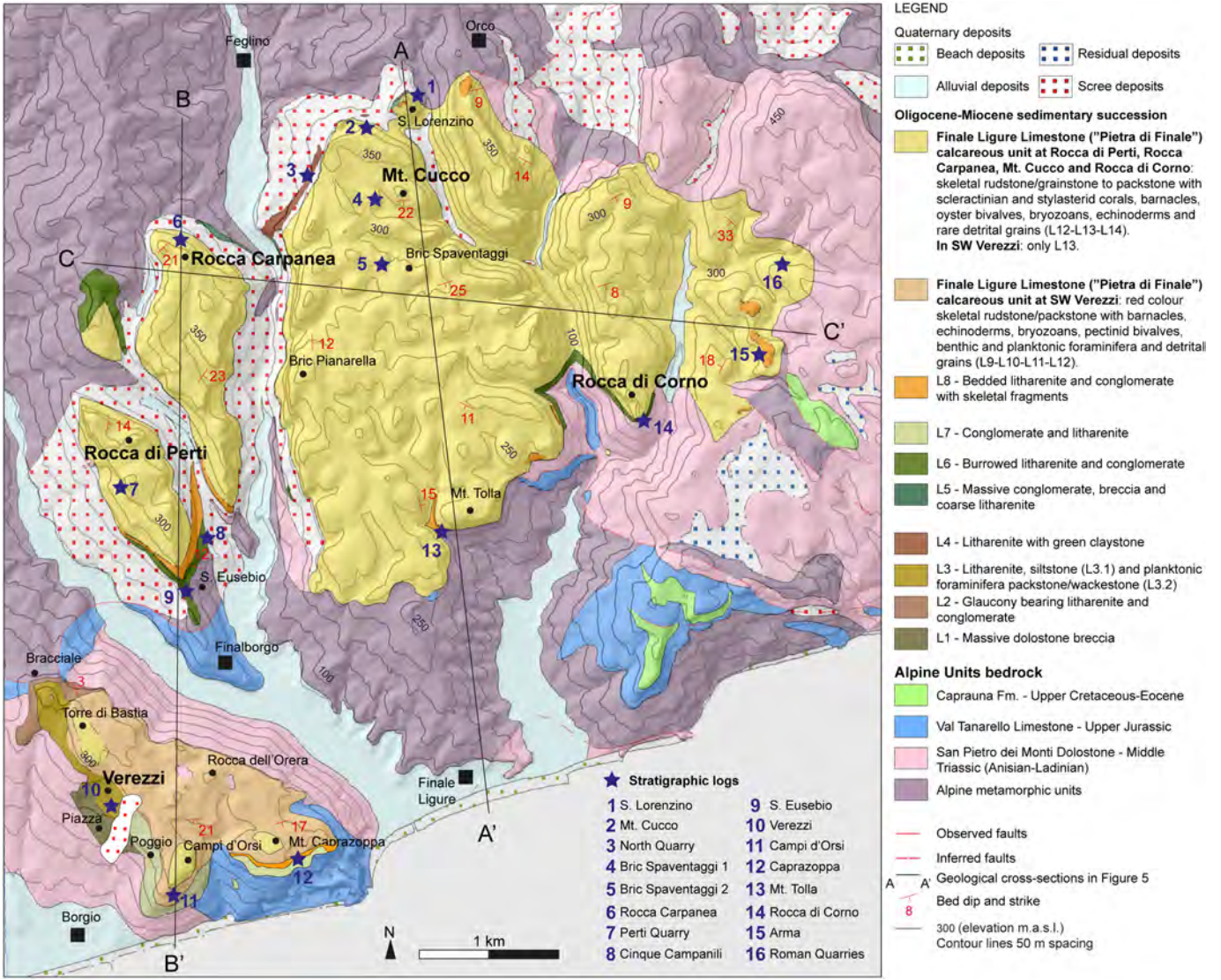
LEGEND
Quaternary deposits
Beach deposits
Residual deposits
Alluvial deposits
Scree deposits
Oligocene-Miocene sedimentary succession
Finale Ligure Limestone ("Pietra di Finale") calcareous unit at Rocca di Perti, Rocca Carpanea, Mt. Cucco and Rocca di Corno: skeletal rudstone/grainstone to packstone with scleractinian and stylasterid corals, barnacles, oyster bivalves, bryozoans, echinoderms and rare detrital grains (L12-L13-L14).
In SW Verezzi: only L13.
Finale Ligure Limestone ("Pietra di Finale") calcareous unit at SW Verezzi: red colour skeletal rudstone/packstone with barnacles, echinoderms, bryozoans, pectinid bivalves, benthic and planktonic foraminifera and detrital grains (L9-L10-L11-L12).
L8 - Bedded litharenite and conglomerate with skeletal fragments
L7 - Conglomerate and litharenite
L6 - Burrowed litharenite and conglomerate
L5 - Massive conglomerate, breccia and coarse litharenite
L4 - Litharenite with green claystone
L3 - Litharenite, siltstone (L3.1) and planktonic foraminifera packstone/wackestone (L3.2)
L2 - Glaucony bearing litharenite and conglomerate
L1 - Massive dolostone breccia
Alpine Units bedrock
Caprauna Fm. - Upper Cretaceous-Eocene
Val Tanarello Limestone - Upper Jurassic
San Pietro dei Monti Dolostone - Middle Triassic (Anisian-Ladinian)
Alpine metamorphic units
Observed faults
Inferred faults
A A' Geological cross-sections in Figure 5
8 Bed dip and strike
300 (elevation m.a.s.l.) Contour lines 50 m spacing
Stratigraphic logs
1 S. Lorenzino
2 Mt. Cucco
3 North Quarry
4 Bric Spaventaggi 1
5 Bric Spaventaggi 2
6 Rocca Carpanea
7 Perti Quarry
8 Cinque Campanili
9 S. Eusebio
10 Verezzi
11 Campi d'Orsi
12 Caprazoppa
13 Mt. Tolla
14 Rocca di Corno
15 Arma
16 Roman Quarries
Feglino
Orco
S. Lorenzino
Mt. Cucco
Rocca Carpanea
Bric Spaventaggi
Bric Pianarella
Rocca di Corno
Rocca di Perti
Mt. Tolla
S. Eusebio
Finalborgo
Bracciale
Torre di Bastia
Rocca dell'Orera
Verezzi
Piazza
Poggio
Campi d'Orsi
Mt. Caprazoppa
Finale Ligure
Borgio
A
A'
B
B'
C
C'
N
1 km

Figure 4

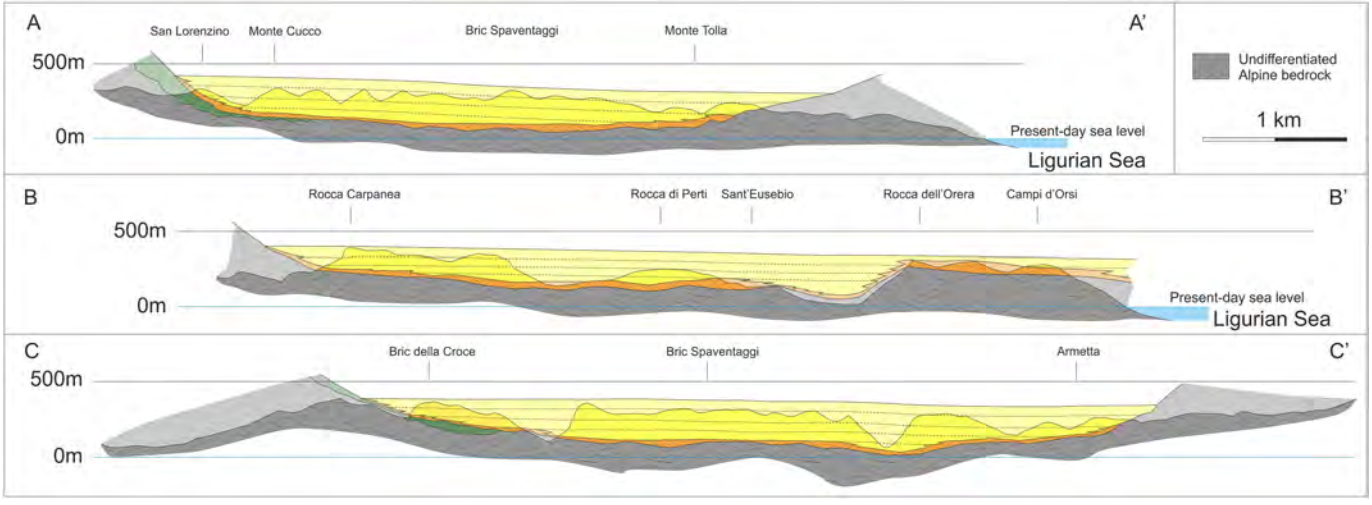
A
San Lorenzino
Monte Cucco
Bric Spaventaggi
Monte Tolla
A'
500m
0m
Present-day sea level
Ligurian Sea
Undifferentiated
Alpine bedrock
1 km
B
Rocca Carpanea
Rocca di Perti
Sant'Eusebio
Rocca dell'Orera
Campi d'Orsi
B'
500m
0m
Present-day sea level
Ligurian Sea
C
Bric della Croce
Bric Spaventaggi
Armetta
C'
500m
0m

Figure 5

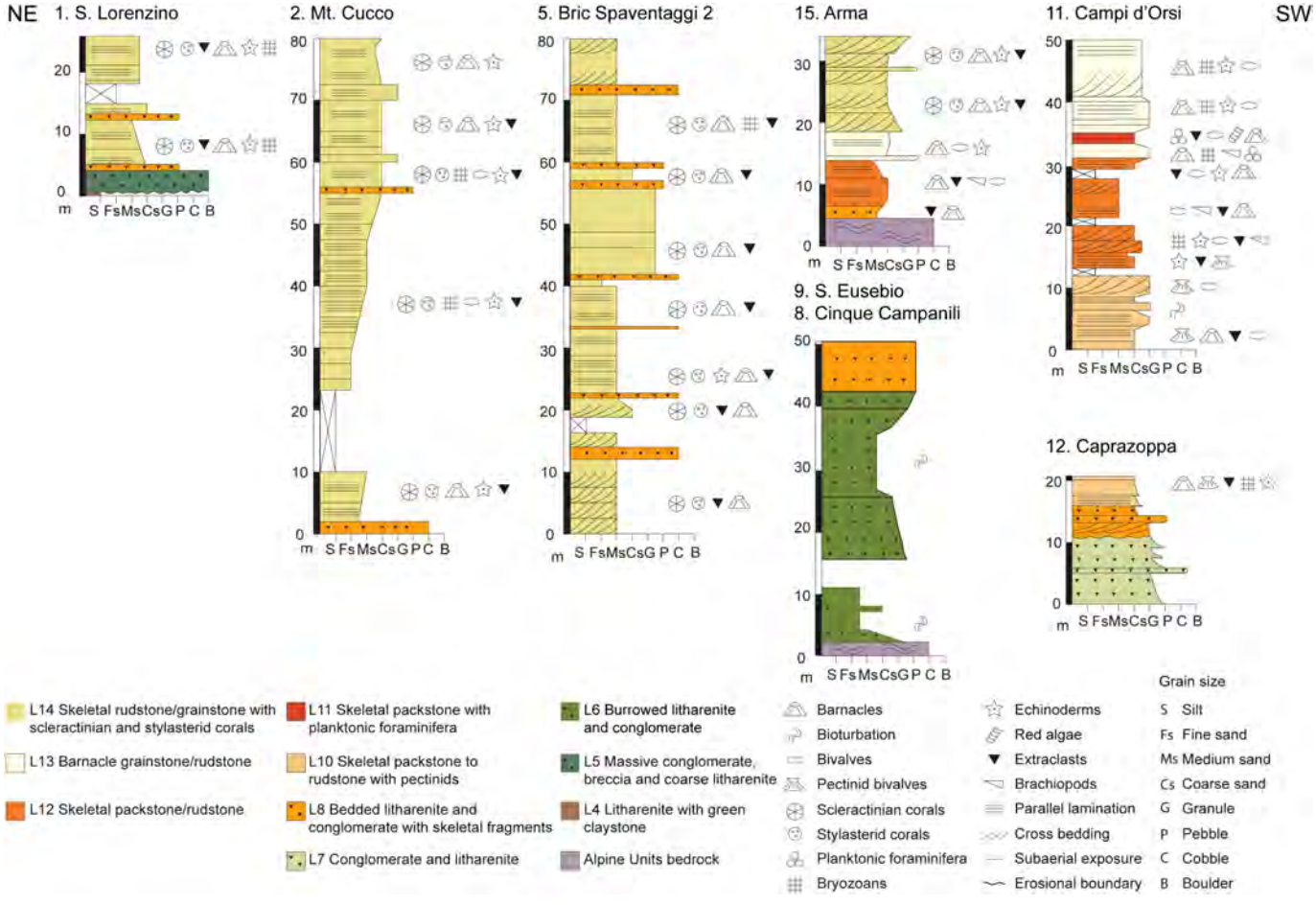
NE
1. S. Lorenzino
2. Mt. Cucco
5. Bric Spaventaggi 2
15. Arma
11. Campi d'Orsi
SW
9. S. Eusebio
8. Cinque Campanili
12. Caprazoppa
m
S Fs Ms Cs G P C B
L14 Skeletal rudstone/grainstone with scleractinian and stylasterid corals
L13 Barnacle grainstone/rudstone
L12 Skeletal packstone/rudstone
L11 Skeletal packstone with planktonic foraminifera
L10 Skeletal packstone to rudstone with pectinids
L8 Bedded litharenite and conglomerate with skeletal fragments
L7 Conglomerate and litharenite
L6 Burrowed litharenite and conglomerate
L5 Massive conglomerate, breccia and coarse litharenite
L4 Litharenite with green claystone
Alpine Units bedrock
Barnacles
Bioturbation
Bivalves
Pectinid bivalves
Scleractinian corals
Stylasterid corals
Planktonic foraminifera
Bryozoans
Echinoderms
Red algae
Extraclasts
Brachiopods
Parallel lamination
Cross bedding
Subaerial exposure
Erosional boundary
Grain size
S Silt
Fs Fine sand
Ms Medium sand
Cs Coarse sand
G Granule
P Pebble
C Cobble
B Boulder

Figure 6

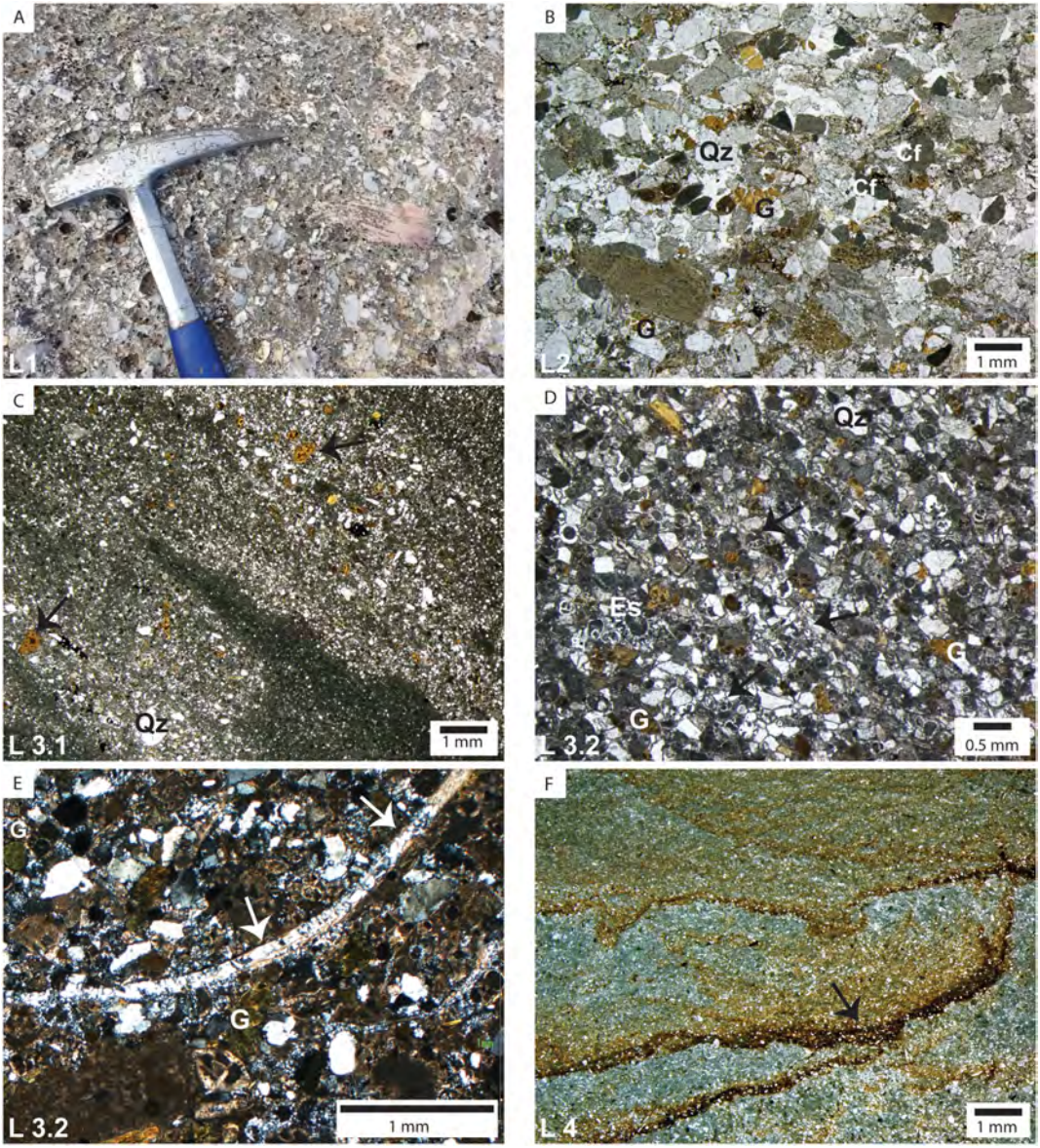
A
L1
B
Qz
Cf
Cf
G
G
L2
1 mm
C
Qz
L 3.1
1 mm
D
Qz
Es
G
G
L 3.2
0.5 mm
E
G
G
L 3.2
1 mm
F
L 4
1 mm

Figure 7

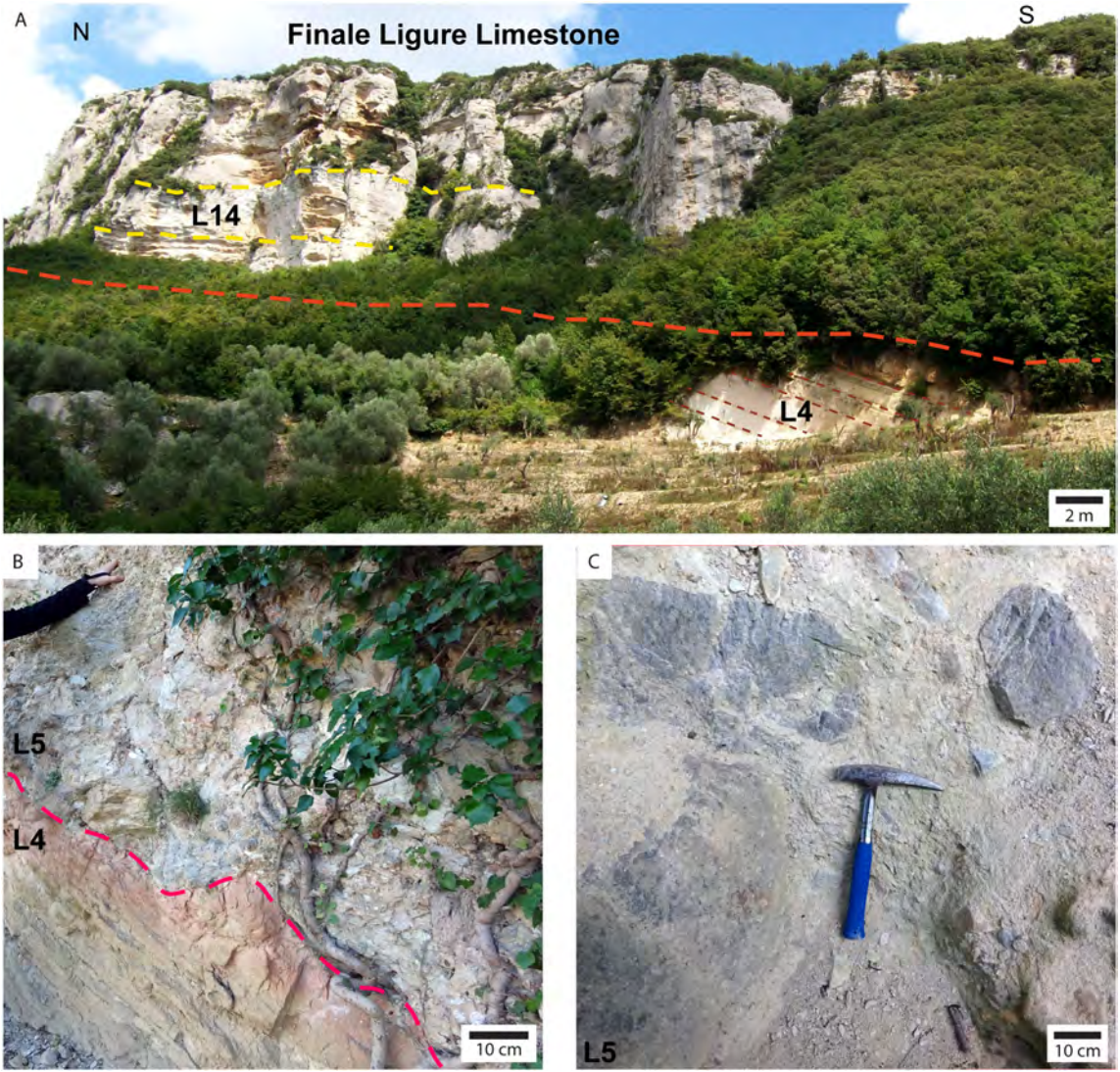

Figure 8

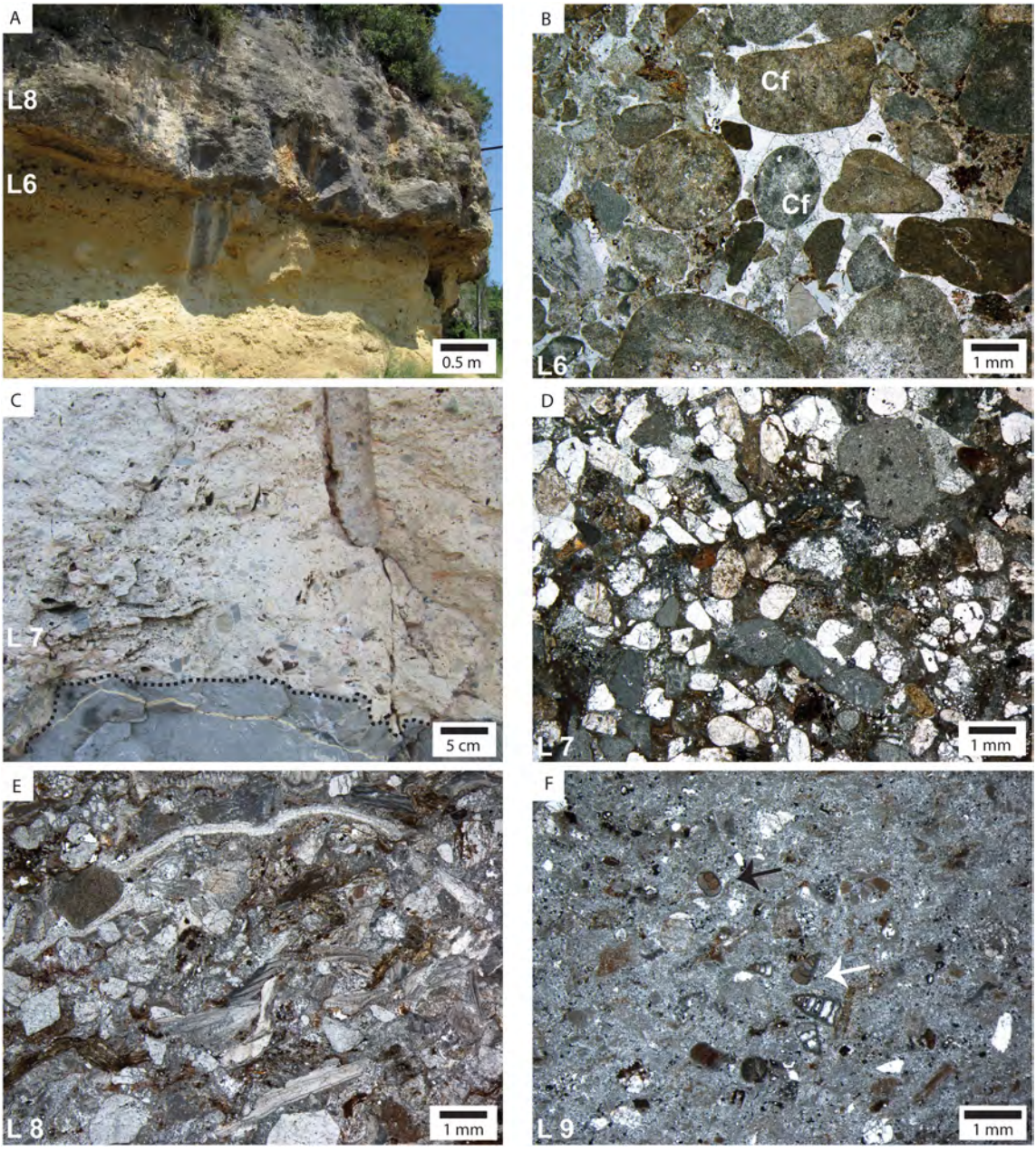

Figure 9

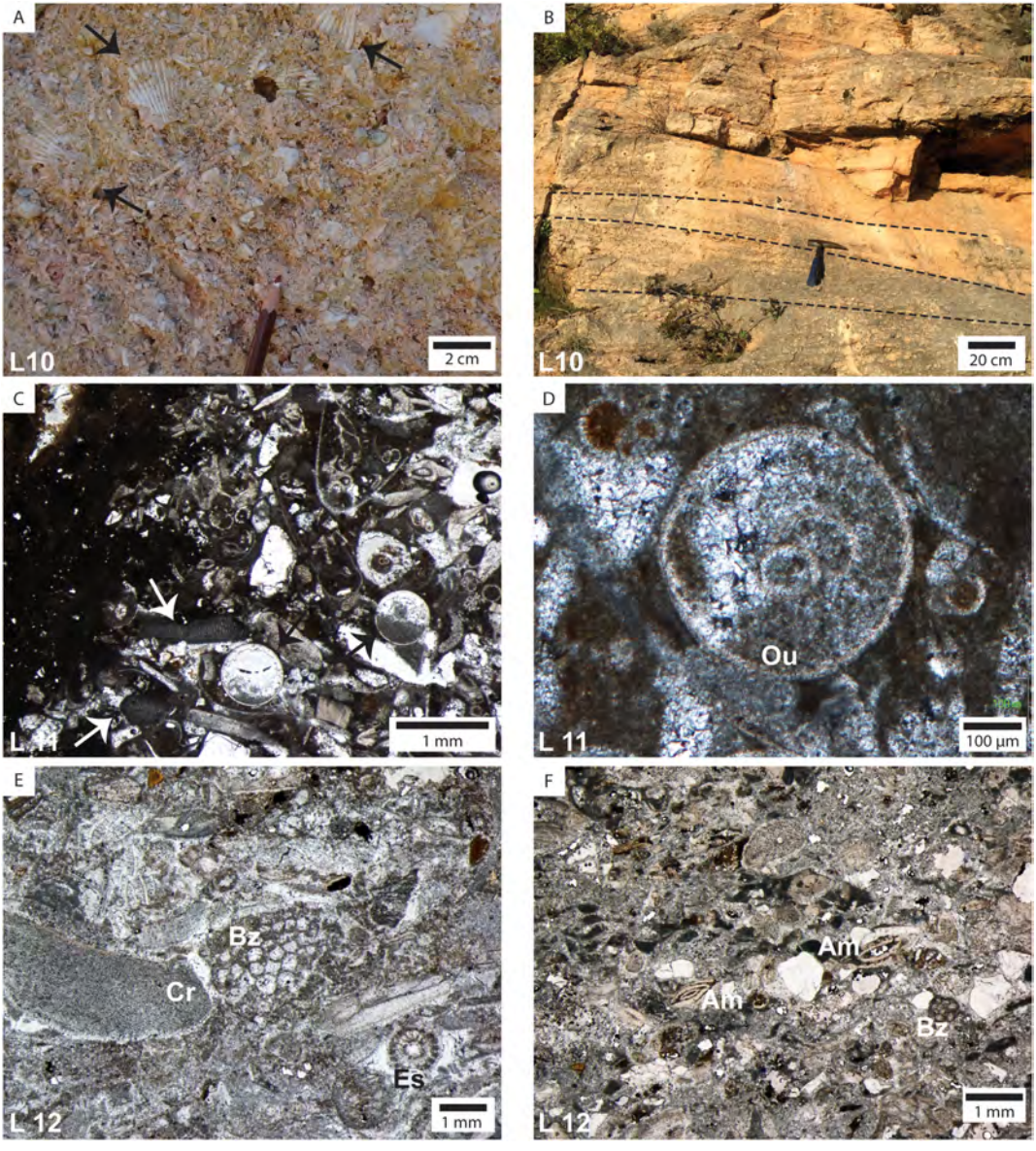
A
L10
2 cm
B
L10
20 cm
C
L 11
1 mm
D
Ou
L 11
100 µm
E
Bz
Cr
Es
L 12
1 mm
F
Am
Am
Bz
L 12
1 mm

Figure 10

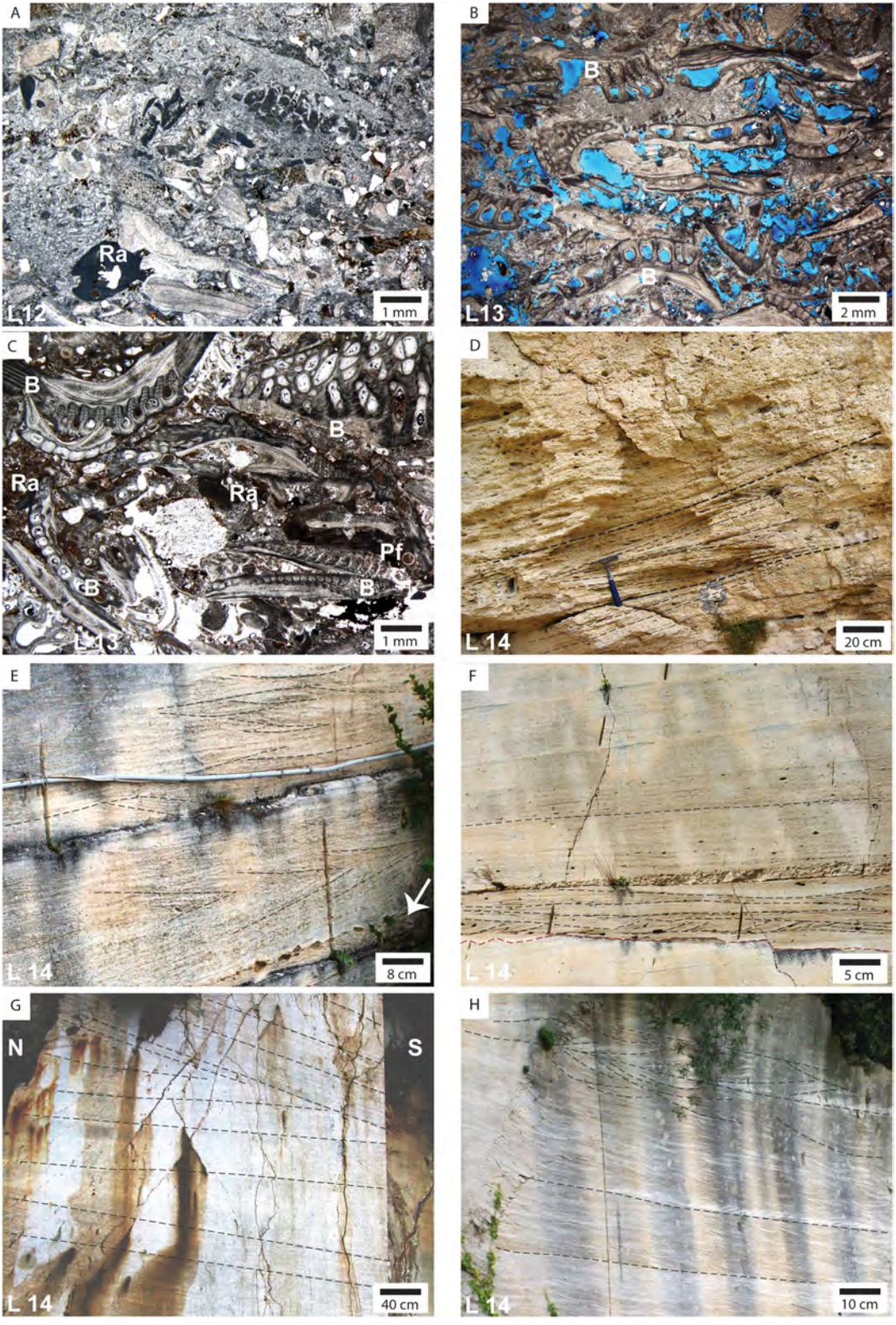
A
Ra
L12
1 mm
B
B
B
L13
2 mm
C
B
B
B
Ra
Ra
Pf
B
B
L13
1 mm
D
L 14
20 cm
E
L 14
8 cm
F
L 14
5 cm
G
N
S
L 14
40 cm
H
L 14
10 cm

Figure 11

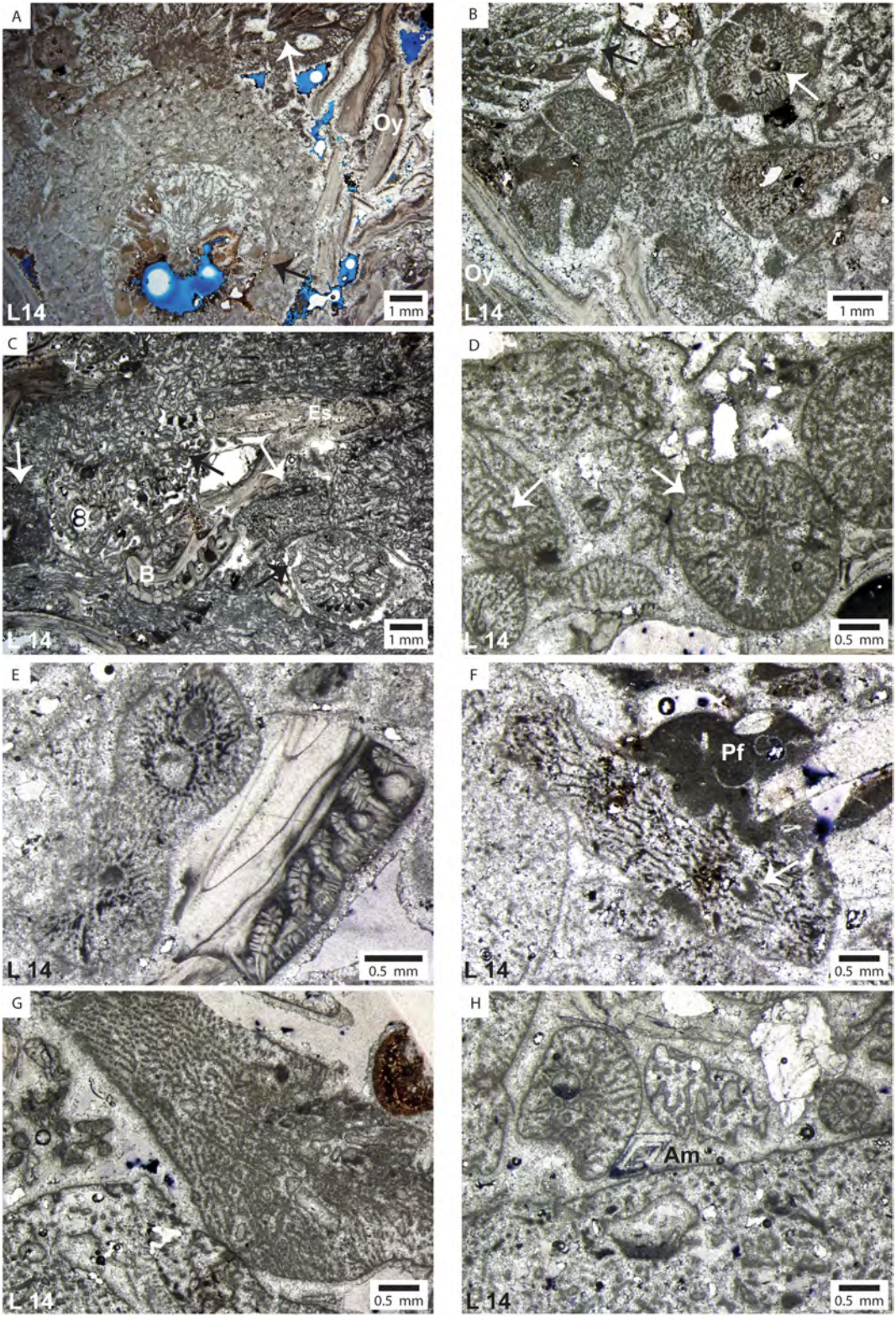
A
Oy
L14
1 mm
B
Oy
L14
1 mm
C
Es
B
L 14
1 mm
D
L 14
0.5 mm
E
L 14
0.5 mm
F
Pf
L 14
0.5 mm
G
L 14
0.5 mm
H
Am
L 14
0.5 mm

Figure 12

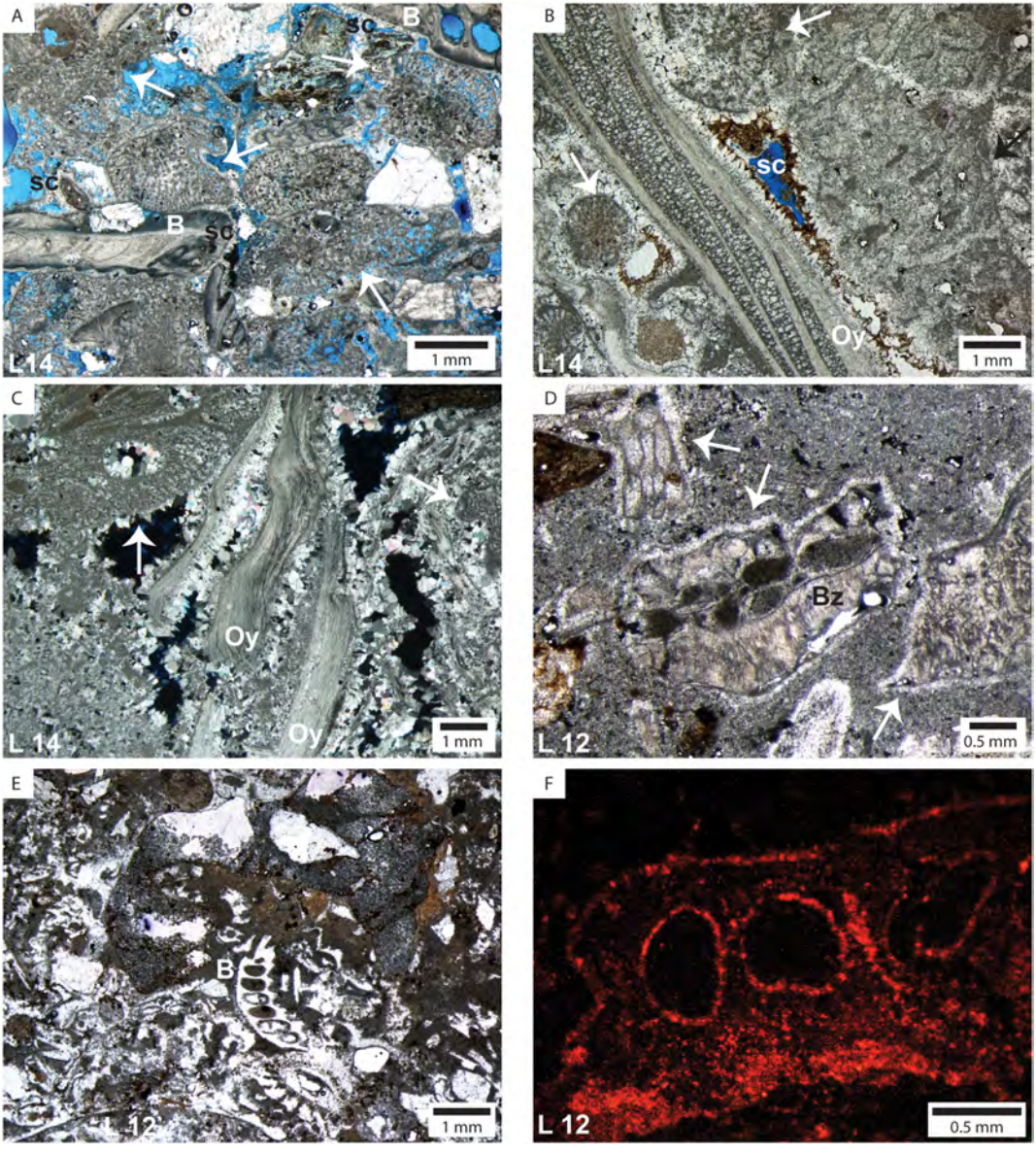
A
B
SC
SC
B
SC
L14
1 mm
B
SC
Oy
L14
1 mm
C
Oy
Oy
L 14
1 mm
D
Bz
L 12
0.5 mm
E
B
L 12
1 mm
F
L 12
0.5 mm

Figure 13

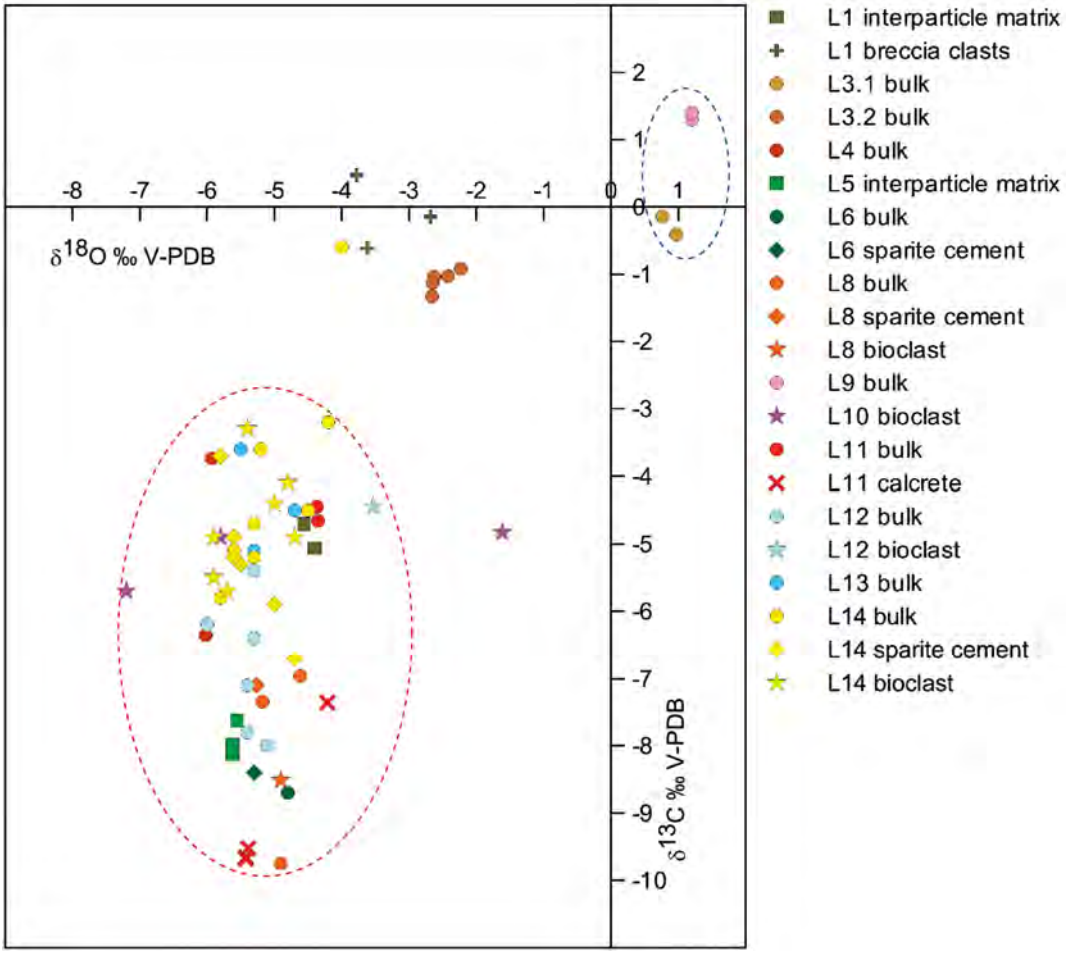
L1 interparticle matrix
L1 breccia clasts
L3.1 bulk
L3.2 bulk
L4 bulk
L5 interparticle matrix
L6 bulk
L6 sparite cement
L8 bulk
L8 sparite cement
L8 bioclast
L9 bulk
L10 bioclast
L11 bulk
L11 calcrete
L12 bulk
L12 bioclast
L13 bulk
L14 bulk
L14 sparite cement
L14 bioclast
δ18O ‰ V-PDB
δ13C ‰ V-PDB
-8
-7
-6
-5
-4
-3
-2
-1
0
1
2
-1
-2
-3
-4
-5
-6
-7
-8
-9
-10

Figure 14

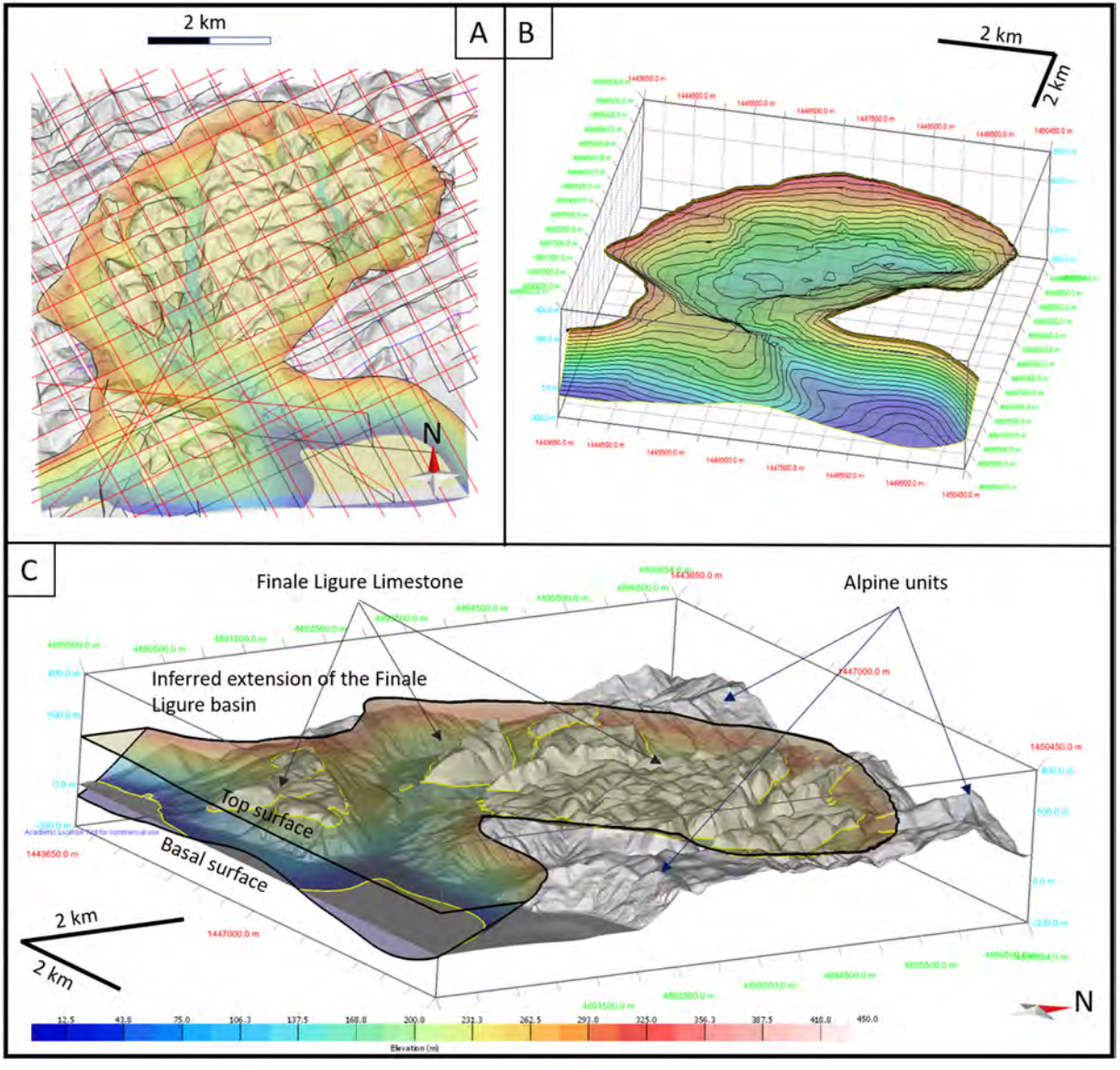
A
2 km
N
B
2 km
2 km
C
Finale Ligure Limestone
Alpine units
Inferred extension of the Finale Ligure basin
Top surface
Basal surface
2 km
2 km
N
Elevation (m)

Figure 15